ESTIMATION OF BRAIN VOLUME FOR DEMENTIA PATIENTS USING MRI

Submitted by

PRASHASTI KANIKAR

(Roll No. P004)

Supervisors

DR. MANOJ S. SANKHE (GUIDE)

DR. DEEPAK P. PATKAR (CO-GUIDE)

for the award of the degree

of

DOCTOR OF PHILOSOPHY (Engineering)

MUKESH PATEL SCHOOL OF TECHNOLOGY MANAGEMENT & ENGINEERING
SVKM's NARSEE MONJEE INSTITUTE OF MANAGEMENT STUDIES (Declared as Deemed-to-be University Under Section 3 of the UGC Act, 1956)
V. L. Mehta Road, Vile Parle (West)
MUMBAI - 400056

(October 2022)

MUKESH PATEL SCHOOL OF TECHNOLOGY MANAGEMENT & ENGINEERING

SVKM's NARSEE MONJEE INSTITUTE OF MANAGEMENT STUDIES
(Declared as Deemed-to-be University Under Section 3 of the UGC Act. 1956)

DECLARATION BY THE CANDIDATE

I, the undersigned hereby declare that the thesis entitled: **Estimation of Brain Volume for Dementia Patients using MRI** for the Award of the degree of Doctor of Philosophy (Engineering) is my own work carried out during the course of study at the university and that to the best of my knowledge and belief, it contains no material previously published or written by another person nor material which has been accepted for the award of any other degree or diploma of the university of India or abroad, except where due acknowledgment has been made in the text.

Name: Prashasti Kanikar
SAP. No.: 70821015004
Mukesh Patel School of Technology Management & Engineering

Date:
Place: Mumbai

MUKESH PATEL SCHOOL OF TECHNOLOGY MANAGEMENT & ENGINEERING
SVKM's NARSEE MONJEE INSTITUTE OF MANAGEMENT STUDIES
(Declared as Deemed-to-be University Under Section 3 of the UGC Act. 1956)

CERTIFICATE BY THE SUPERVISOR AND GUIDE

This is to certify that the thesis entitled: **Estimation of Brain Volume for Dementia Patients using MRI** submitted by **Prashasti Kanikar** with SAP No. **70821015004** to the University for the Award of the degree of Doctor of Philosophy (Engineering) is a bonafide record of the research work carried out by him under my supervision and guidance. The content of the thesis, in full or parts have not been submitted to any other Institute of University for the award of any other degree or diploma.

Research Supervisor and Guide

1. _____
Signature

Name : Dr. Manoj S. Sankhe

2. _____
Signature

Name : Dr. Deepak P. Patkar

Date:
Place: Mumbai

Forwarded by the Dean of the School

Dr. Alka Mahajan
(Dean, MPSTME)
Mukesh Patel School of Technology Management and Engineering

MUKESH PATEL SCHOOL OF TECHNOLOGY MANAGEMENT & ENGINEERING

SVKM's NARSEE MONJEE INSTITUTE OF MANAGEMENT STUDIES

(Declared as Deemed-to-be University Under Section 3 of the UGC Act, 1956)

CERTIFICATE OF EXAMINING COMMITTEE

This is to certify that the thesis entitled: **Estimation of Brain Volume for Dementia Patients using MRI** prepared by **Prashasti Kanikar** complies with the University regulations and that it meets the accepted standards with respect to originality and quality.

For the Award of degree of **Doctor of Philosophy (Engineering)**

Signed by the final examining committee:

_____

_____

Signed by the Supervisors and Guide

_____

Signed by the Dean of School:

_____

To the librarian:

This thesis is not to be regarded as confidential.

_____

Professor In-charge of the thesis

ACKNOWLEDGEMENTS

I would like to express my gratitude to my mentor Dr. Manoj S. Sankhe for his unwavering support and guidance throughout my research duration. This thesis would not have been possible without his guidance and resourcefulness.

I would also like to extend my gratitude to Dr. Deepak P. Patkar for his valuable contribution in the development of my thesis. He has helped me in understanding the current clinical approach and in understanding Imaging data. His knowledge and insights have greatly enhanced my experience in the field.

I would also like to express my thanks to Dr. Mitusha Verma and Dr. Gauri Ahuja for their valuable contributions in the development of my thesis. They helped me create a gold standard ground truth for this study.

I would also like to thank Dr. Alka Mahajan, Dean, Mukesh Patel School of Technology Management and Engineering, SVKM's NMIMS for lending her support.

I want to express my heartfelt gratitude to my parents, siblings, family and friends for giving me valuable suggestions, helping and motivating me during my PhD.

Finally, I would like to thank Suhas, my husband for his support throughout my research period. I render a big thank to my son Darsh, without whose motivation I could not complete this work.

ABSTRACT

Keywords: Brain Volume Estimation, Brain Tissue Segmentation, Dementia Classification

The estimation of brain volume is a challenging area in the medical domain. It is very important to understand the volume of the brain in order to track the progression of various brain diseases. This study aims to develop a method that can be used to estimate the brain volume using MRI (Magnetic Resonance Imaging) data. Two models are proposed using different gradient filters for estimation of Intra-Cranial Volume (ICV) and Total Brain Volume (TBV) .

First, a novel approach for estimation of ICV is presented. The study was conducted on the data collected from the Nanavati Hospital and the Open Access Imaging Studies (OASIS) database. The proposed method was able to achieve an average accuracy of 94.19% for OASIS data and 93.4% for Nanavati hospital data. This method can help in the diagnosis and monitoring of neurodegenerative diseases.

Secondly, a model for estimation of Total Brain Volume using Mutiplicative Intrinsic Component Optimization (MICO) is proposed. In this model, it is tried to address intensity inhomogeneity problem by correction of bias field and then segmentation of tissues like Gray Matter (GM), White Matter (WM) and Cerebrospinal Fluid (CSF). This leads to calculation of Total Brain Volume (TBV). The proposed model performs better than MICO algorithm for both OASIS dataset and on data from Nanavati Hospital.

Due to the effects of dementia, one's cognitive function can decline in various areas, such as memory and language. It is therefore important that a model is created that can predict its occurrence and its progression. This can help prevent it from happening in the first place. One of the most effective ways to diagnose and monitor this condition is through the use of neuroimaging. This study aims to find the best machine learning algorithm for analyzing neuroimaging data. The IBK Algorithm performed the best with an accuracy of 98.93%. It was validated using the OASIS dataset.

TABLE OF CONTENTS

ABSTRACT vi
TABLE OF CONTENTS vii
LIST OF FIGURES ix
ABBREVIATIONS xi
LIST OF TABLES xii

CHAPTER 1 1

INTRODUCTION 1

1.1.INTRODUCTION 1
1.2.OBJECTIVE OF THE WORK 2
1.3.PROBLEM DEFINITION 2

CHAPTER 2 3

LITERATURE REVIEW 3

2.1.INTRODUCTION 3
2.2.HUMAN BRAIN 4
2.3.DEMENTIA 5
2.4.MAGNETIC RESONANCE IMAGING 7
2.5. VOLUME ESTIMATION AND ANALYSIS 7
2.6.BRAIN TISSUE SEGMENTATION APPROACHES USING BIAS FIELD CORRECTION 8
2.7.MANUAL METHOD FOR BRAIN VOLUME MEASUREMENT 9
2.8.AUTOMATED APPROACHES FOR BRAIN VOLUME ESTIMATION 9
2.9.SKULL STRIPPING 9

CHAPTER 3 10

ESTIMATION OF INTRACRANIAL VOLUME 10

3.1.COMPONENTS OF PROPOSED MODEL 10
3.2.SOURCES OF DATA 13
3.3.PROPOSED MODEL FOR INTRACRANIAL VOLUME ESTIMATION 15
3.4.PERFORMANCE EVALUATION PARAMETERS 16
3.5.RESULTS 16
3.6.SUMMARY 23

CHAPTER 4.....24

ESTIMATION OF TOTAL BRAIN VOLUME 24

4.1.INTRODUCTION..... 24

4.2.PROPOSED MODEL FOR ESTIMATION OF TOTAL BRAIN VOLUME 25

4.3.RESULTS 26

4.4. COMPARATIVE ANALYSIS OF RESULTS 27

4.5.TIME ESTIMATION OF ICV AND TBV TOGETHER 30

4.6.SUMMARY..... 30

CHAPTER 5.....31

DEMENTIA CLASSIFICATION 31

5.1.INTRODUCTION..... 31

5.2.MACHINE LEARNING BASED APPROACHES 31

5.3.MORE CLASSIFIERS 32

5.4.RESULTS 34

5.5.SUMMARY..... 38

CHAPTER 6.....39

CONCLUSION & FUTURE SCOPE 39

6.1.CONCLUSION 39

6.2.FUTURE SCOPE 40

PUBLICATIONS.....41

REFERENCES.....42

LIST OF FIGURES

Fig. 2.1: Concept Map-I for Literature Review……..……....3
Fig. 2.2: Concept Map-II for Literature Review……..……..…….4
Fig. 2.3: Human brain showing various tissue classes on a coronal slice…….……..5
Fig. 2.4: Types of Dementia……..…...…..6
Fig. 2.5: Types of approaches used for bias field correction…..……..……8
Fig. 3.1: Volume Refinement…….……..……..12
Fig.3.2: MRI volumetric data of a 65 year old male subject……...…..14
Fig.3.3: Proposed model for Brain Volume estimation……..…..15
Fig.3.4: Images after execution of different steps in proposed model with GMIF for s-I…...…17
Fig.3.5: Images after execution of different steps in proposed model with GMRG Filtering….18
Fig.3.6: Images after execution of different steps in proposed model with GAD Filtering……19
Fig.3.7: Brain Volume estimation accuracies using OASIS and Nanavati data……...….21
Fig.3.8: RMSE of Proposed models using using OASIS and Nanavati data…….…….....21
Fig.3.9: Scatter Indices of Proposed models using using OASIS and Nanavati data……22
Fig.3.10: Average ICV estimation time for Proposed models using OASIS and Nanavati data22
Fig.3.11: Comparison Proposed models with other methods for estimation of Brain volume .23
Fig. 4.1: Proposed model for estimation of Total Brain Volume……...25
Fig.4.2: Images after execution of different steps in proposed model with GMIF for s-I……..26
Fig.4.3: Comparison of TBV estimation accuracies by proposed model with MICO……....28
Fig.4.4: Comparison of RMSE of Proposed models with MICO……..…..…..28
Fig.4.5: Comparison of Scatter Indices of Proposed models with MICO……..29
Fig.4.6: Comparison of TBV estimation time for Nanavati and OASIS dataset……..…29
Fig.4.7: Comparison of estimation time for ICV and TBV together…….……30
Fig.5.1: Classifiers used for comparison……..…32
Fig.5.2: Graph showing % of correctly classified instances…….…….36
Fig.5.3: Graph showing True Positive and False Positive rates for top 10 algorithms…..……37

ABBREVIATION NOTATION AND NOMENCLATURE

ACM - Active Contour Model

ASF - Atlas Scaling Factor

DICOM - Digital Imaging and Communication in Medicine

EHR -Electronic Health Records

GAD- Gradient Anisotropic Diffusion

GB - Gradient Boosting

GMIF- Gradient Magnitude Image Filter

GMRGIF- Gradient Magnitude Recursive Gaussian Image Filter

ICV - Intra-Cranial Volume

ITK - Insight Segmentation and Registration Toolkit

k-CV - k-fold Cross-Validation

k-NN - k-Nearest Neighbour

LDA - Linear Discriminant Analysis

MICO-Mutiplicative Intrinsic Component Optimization

MRI - Magnetic Resonance Imaging

MSE - Mean Squared Error

NMR - Nuclear Magnetic Resonance

OASIS - Open Access Series of Imaging Studies

RMSE - Root Mean Squared Error

ROI - Region of Interest

SVM - Support Vector Machines

T1-W - T1 Weighted

TBV - Total Brain Volume

VBM - Voxel Based Morphometry

LIST OF TABLES

Table 3.1: Image Attributes……..……..……..13
Table 3.2: Results for Subject OS67 using proposed model with GMI filtering…….……....17
Table 3.3: Results for Subject OS67 using proposed model with GMRG filtering…..…..……18
Table 3.4: Results for Subject OS67 using proposed model with GAD filtering……19
Table 3.5: Performance evaluation metrics for OASIS dataset…….....20
Table 3.6: Gender-wise count of Subjects in Nanavati dataset……..…..20
Table 3.7: Performance evaluation metrics for Nanavati dataset……..20
Table 4.1: Results of proposed model for TBV estimation for subject OS67…….27
Table 4.2: Performance evaluation metrics for OASIS dataset…….....27
Table 4.3: Performance evaluation parameters for proposed models using Nanavati dataset...27
Table 5.1: Accuracies of Dementia Prediction Models……..…35
Table 5.2: Detailed classification results…….…..35
Table 5.3: Detailed results with different parameters…….……..36
Table 5.4: Detailed results of IBk classifier…….……37
Table 5.5: Confusion Matrix for IBk classifier……38

CHAPTER 1

INTRODUCTION

1.1. INTRODUCTION

The estimation of brain volume is a challenging area in the medical domain. It is very important for the diagnosis and monitoring of various brain diseases. According to Liu et. al., Brain volume loss associated with very early Dementia can be detected by MRI (Magnetic Resonance Imaging), even before cognitive symptoms appear[1]. Radiologists have been fascinated by the size, shape, and volume of the skull since the beginning. Magnetic resonance imaging can be used to determine the total brain volume. This is an important parameter in the evaluation of neuropsychiatric and neurological disorders. One of the most common types of disorders that can be characterized by brain volume loss is Alzheimer's disease[2].

The development of dementia is a terminal illness that affects people with age as they grow older. The related symptoms are memory loss and poor judgment. It is a major public health issue that affects the people with aging. The WHO (World Health Organization) states that every three seconds, someone in the world gets diagnosed with dementia. Around 55 million people globally are affected by this disease. By 2050, it is estimated that there will be over 140 million people with this condition[3]. Due to the complexity of the disease, the need for non-invasive methods to diagnose and treat it, is growing. Hence, this study aims to develop an automated method for estimating brain volume using MRI data.

Various methods have been proposed to analyze and detect Alzheimer's disease using Brain imaging data. Most of these methods utilize neuroanatomical biomarkers to describe the physiological properties of the affected brain regions, such as the hippocampus. The most common automated methods used in this field are summarized in literature review chapter. This study aims to analyze the various scenarios of the use of MRI-based brain volumetry in the diagnosis and monitoring of neurological disorders. It can help in supporting disease diagnosis, monitoring treatment response, understanding mechanisms and tracking clinical progression of diseases.

1.2. OBJECTIVE OF THE WORK

This study aims to develop models for estimation of brain volume, which in turn can help radiologists in disease diagnosis and tracking clinical progression of brain related diseases like Dementia. This study is also helpful in pharmaceutical research, to compare the effects of new drugs on different populations of patients. The following section lists research objectives formulated in the initial phase of study.

1.3. PROBLEM DEFINITION

Most of the existing methods are time consuming, require human interaction and less accurate in terms of tissue classification. Hence, an accurate method is required for early detection of dementia. This study aims to devise a method for estimation of Brain Volume from MR Images and then predict dementia.

1.3.1. Research Objectives

- To estimate overall Brain Volume (ICV) from appropriate MRI data set
- To classify different types of tissues in atrophy
- To predict dementia

In this report, a brief description of proposed modules is given that addresses above research objectives.

1.3.2. Applications of this study

- Supporting disease diagnosis
- Understanding mechanisms and tracking clinical progression of disease
- In pharmaceutical research, to compare the effects of new drugs on different populations of patients[4]

CHAPTER 2
LITERATURE REVIEW

2.1. INTRODUCTION

In this research various resources such as databases, search engines, and libraries are used to keep the research organized and up to date. All topics related to this research work were studied and summarized in brief to explain general idea and their role in designing the proposed modules.Following fig. 2.1 shows concept map of few topics and subtopics covered in literature review.

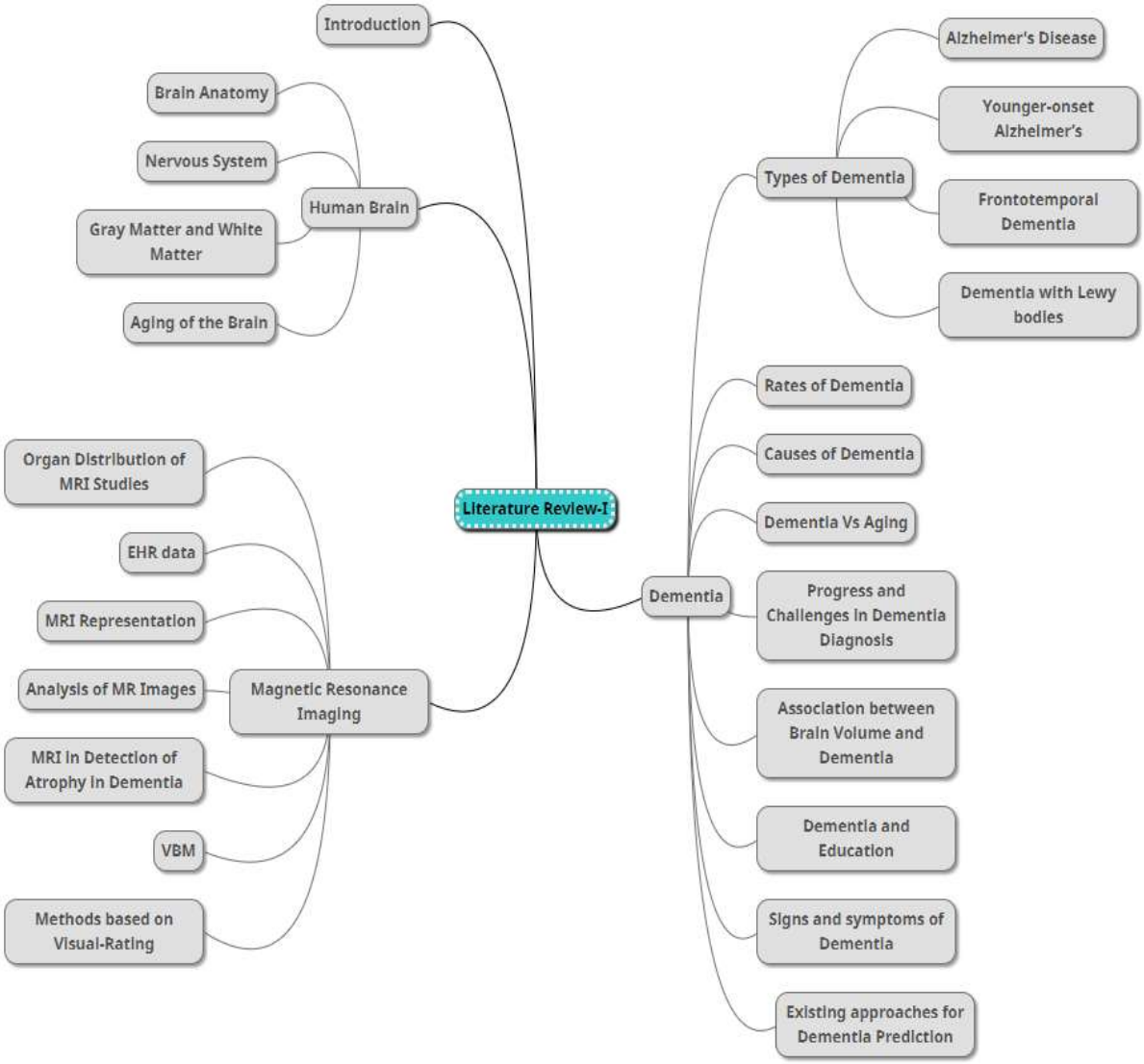

Fig. 2.1: Concept Map-I for Literature Review

Following fig. 2.2 is an extension of fig. 2.1. It shows concept map of remaining topics and subtopics covered in literature review.

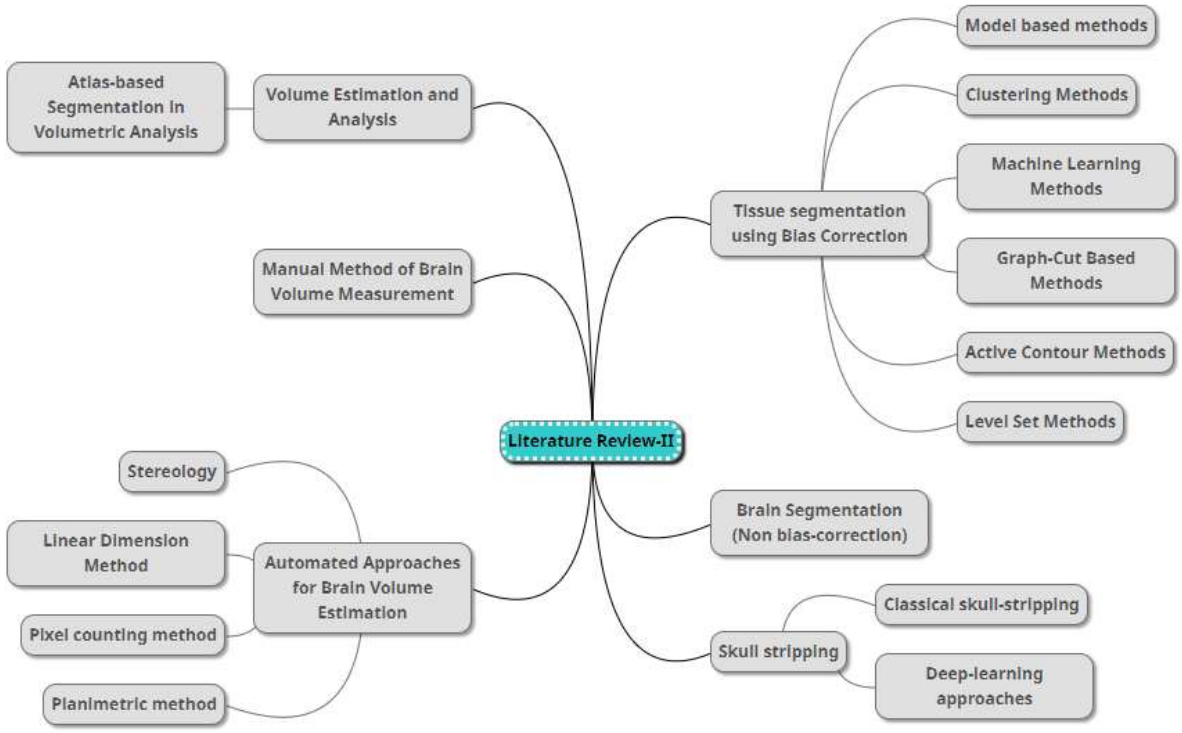

Fig. 2.2: Concept Map-II for Literature Review

2.2. HUMAN BRAIN

2.2.1. Brain anatomy

Understanding of the brain is regarded as one of the last frontiers of human knowledge. For decades, in neuroscience, various components of the nervous system are being studied. One of these is the brain, which is responsible for controlling the rest of the body.

2.2.2. Nervous system

The human brain along with the spinal cord constitutes the central nervous system of the body. It consists of three major components: the cerebrum, the cerebellum and the brainstem. Without the nervous system, our bodies can't function properly.

2.2.3. Gray matter and white matter

Following fig. 2.3 shows representational drawing of human brain showing various tissue classes, including the white matter and gray matter, and the ventricles, which are composed of cerebrospinal fluid shown on a coronal slice[6]

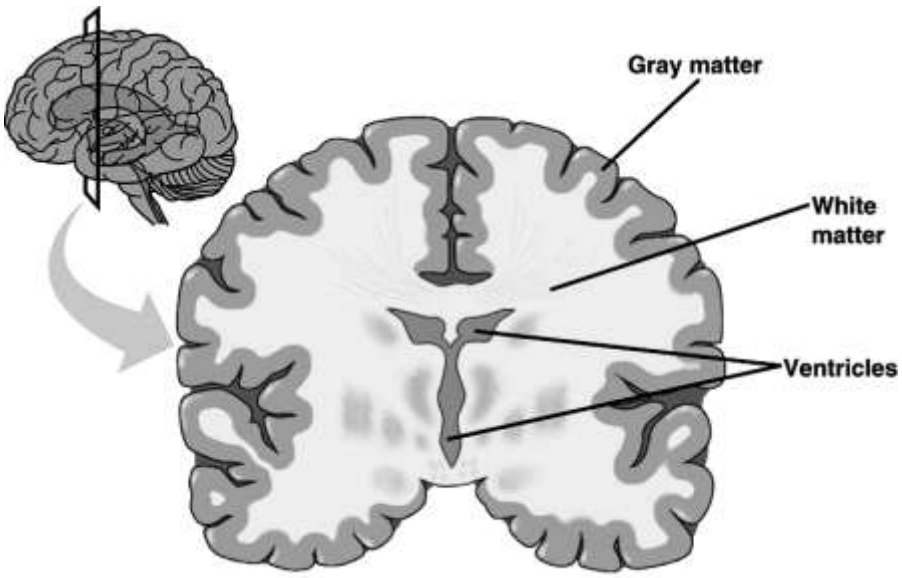

Fig. 2.3: Human brain showing various tissue classes on a coronal slice (Source [6])

2.2.4. Aging of the Brain

As people get older, the number of neurons in their brain decreases. This phenomenon is not noticeable, as the remaining neurons can still function properly to compensate for the loss. It is believed that the brain gradually loses weight over time, and this could happen between the age of 20 and 90.

2.3. DEMENTIA

The umbrella term dementia refers to a collection of symptoms that are caused by various conditions that affect the functioning of the brain. Some of these include memory loss, behavior, and language. The most common type of dementia is Alzheimer's disease. Other types include frontotemporal dementia and vascular dementia. Following fig. 2.4 shows different types of dementia.

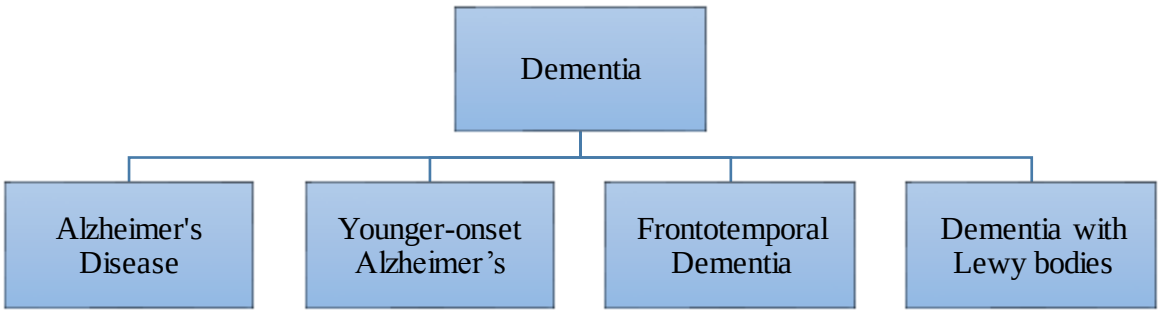

Fig. 2.4: Types of Dementia

2.3.1. Association between Brain Volume and Dementia

There are also various age-related changes that can affect the brain's volume. However, in normal aging, these changes are relatively minor and can be attributed to the aging process. On the other hand, in disease states, the volume loss is greater than can be explained by age [2].

2.3.2. Existing approaches for Dementia Prediction

Machine learning has demonstrated promising applications to neuroimaging data analysis for dementia prediction and care[12].Patil and Yardi have proposed ANN based approach for Dementia Diagnosis. The steps include intensity computation, discrete cosine transform application for extracting features and classification using supervised neural network [13].Yo-Ping Huang et al. have proposed Fuzzy inference based approach using MRI data. The system is able to monitor separately left and right brain hemispheres and possible outcomes are MCI, Healthy or schizophrenia[14]. Gunawardena et al. have proposed a Support Vector Machine based approach for dementia classification. It includes preprocessing, Region of Interest (ROI) selection and edge detection. It is a proposed method, results are not published[15]. In a study conducted by Seong-Eun Ryu and colleagues, they proposed a model that uses the XGBoost algorithm to predict the risk of developing dementia.This method gave 85.61% accuracy[16].

H. M. Tarek Ullah et.al. proposed an approach for Dementia detection using Deep Convolutional Neural Networks[17]. Esther E. Bron et.al have proposed an approach for Feature Selection Based on the SVM Weight Vector for Classification of Dementia. The researchers found that the model performed better than the expert knowledge and t-statistics when it came to identifying the most relevant features. They also noted that the method based on the p-map had the highest performance when it came to estimating the relevance of various

feature[18]. Simon Duchesne et al. proposed an automated classification method using computational techniques within the context of cross-sectional analysis of MRI. They achieved accuracy of 92% using a support vector machine[19]. C. Studholme et al. have proposed a direct template-based approach to separating the inhomogeneity of MRI intensity from the tissue-intensity structure. This method resulted better in a global bias estimate[20].

Varun Jain et al. have proposed Augmentation and Classification model based on severity that classifies dementia into various categories. Using MRI scans[21]. Rory Raeper and colleagues developed a novel ensemble classifier-learning framework for early dementia diagnosis using multiple brain structures. Their approach significantly outperformed other state-of-the-art methods[22]. Abol Basher et al. proposed a method to diagnose Alzheimer's disease using slice-wise volumetric features from the left and right hemispheres of the brain. Their method combines a convolutional neural network model and a deep neural network model[23]. A team led by Jian Cheng developed a novel 3D convolutional network that can estimate the brain age from T1weighted MRI data. It can also be used to distinguish between healthy subjects and those with mild cognitive impairment[24].Stephanos Leandrou et al. have reviewed various methods used for the quantitative structural MRI acquisition for the assessment of Alzheimer's disease. The researchers used various methods to analyze the data collected by the study. These included measurements of regions of interests, shape analysis, cortical thickness and Voxel-based morphometry[25].

2.4. MAGNETIC RESONANCE IMAGING

Magnetic resonance imaging is a type of imaging that uses radiofrequency waves to visualize the spinning of hydrogen atoms within the brain. This technique can be used in monitoring and diagnosis of various brain related disorders. Through MRI, researchers can gain quantitative and qualitative information about the tissues in the body.

2.5. VOLUME ESTIMATION AND ANALYSIS

Due to the increasing importance of brain structures analysis, the use of volumetric techniques has become more prevalent. In a study conducted by Henrike Wolf and colleagues, they found that the severity of the cognitive impairment was related to the intracranial volume.[31]. In order to estimate the intracranial volume, Karen J. and colleagues used a single slice's cross-sectional area to calculate the volume. They found that the correlation between the cross-sectional area and the inoculation volume was strong.[32].

According to Eritaia et al., the lack of a reliable method to estimate the non-pathological differences between brain volume has been an issue in previous studies. They identified various factors such as body size, sex, and age as possible causes of these differences.[33]. In a study conducted on the effects of different brain regions on cognitive impairment, I. Driscoll and colleagues discovered that the loss of volume in these regions was associated with mild cognitive impairment.[34].

In a study conducted by Klasson et al., they discovered that the use of the software known as FS was biased by the total brain volume[35]. According to Ridgway et. al. inter-subject variability can be measured by total intracranial volume[36]. Richard N. et al. compared the biases found in the software packages used in the study. They discovered that the use of the software known as FS was biased by the size of the skull. On the other hand, the use of the software known as SPM was biased by the atrophy and gender factors [37].

Currently, the methods used to estimate the brain volume are not very accurate due to the lack of anatomical specificity, time-consuming computation, and erroneous tissue classification.

2.6. BRAIN TISSUE SEGMENTATION APPROACHES USING BIAS FIELD CORRECTION

It is still challenging to extract objects from complex images due to the presence of inhomogeneity and noise in the data[39]. It can reduce the high frequencies of the images, such as the edges and contours, and it changes the intensity of the images so that the same tissue has varying gray level distribution.[40]. The following fig. 2.5 shows different types of approaches used for correction of bias field.

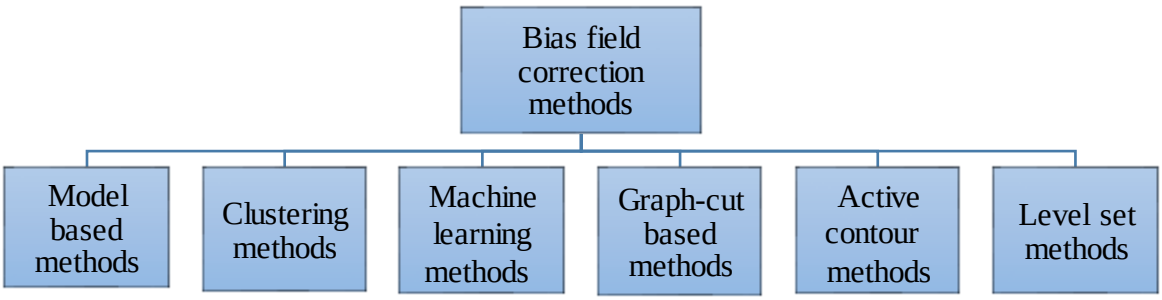

Fig. 2.5: Types of approaches used for bias field correction

Important approaches like-Model based methods[41],[42],Clustering Methods[43],Machine Learning Methods [44], Graph-Cut Based Methods[45],Active Contour Methods [46] are studied.

2.6.1. Level Set Methods

Variety of models include : Chan and Vese [47],Chunming Li [48],LINC algorithm [39] and correntropy-based approach [36].

MICO method decomposes the images to create two multiplicative components: the true image and the bias field. This algorithm for optimizing the bias field is performed iteratively, using efficient matrix computation. It achieves stable and robust results due to the convexity of its formulation[37].

2.7. MANUAL METHOD OF BRAIN VOLUME MEASUREMENT

Despite the time-consuming and rater-dependent nature of the manual method, it is still the gold standard of imaging for assessing the region of interests. [55]. The manual method uses a T1weighted MRI image to draw boundaries of the brain using an in-house software program The volumes are then calculated by taking into account all voxels within the traced area and multiplying by resolution of MRI. Manual tracing of brain boundaries on 3 –Dimensional volumetric data takes around 25 minutes per patient. In this research, it is tried to estimate brain volumes with a decent accuracy in less than 11 minutes time per patient on an average.

2.8. AUTOMATED APPROACHES FOR BRAIN VOLUME ESTIMATION

Variety of automated approaches are proposed to estimate brain volume from MRI images. They are stereology([56],[57]),linear regression technique [58], pixel counting-based technique[60] and Planimetric methods[61].

2.9. SKULL STRIPPING

The process of skull stripping is performed to analyze the medical images of the head. It is very important for various algorithms that perform automatic segmentation and registration of brain images. Unfortunately, most of the time, these methods require a lot of time to perform properly[62]. The models are designed to be supervised, and they use a set of acquired training images to produce accurate and fast models[63].

CHAPTER 3
ESTIMATION OF INTRACRANIAL VOLUME

The measurement of brain volume is very important for various neurological applications. It is typically performed to check the growth and changes of the brain in patients with normal or abnormal conditions. Magnetic Resonance Imaging is a good modality for volume measurement due to its excellent contrast and better image resolution.

3.1. COMPONENTS OF PROPOSED MODEL

3.1.1. Gradient Filters

The gradient of an image provides two pieces of information about how it is changing. One of these is the magnitude of the change, while the other is the direction of the gradient. For instance, if an image is taken at a given height, the gradient will be the direction that it goes up. Similarly, an image in a terrain will have a different direction if it is taken at a different elevation.

The magnitude of the gradient can be used to determine how quickly our height increases when we walk a small step uphill. Since the gradient has both a direction and a magnitude, we can encode this information in vectors. The length of the vector that contains this information determines the gradient's magnitude, while its direction gives it its direction. Because the gradient can vary in its location, we can represent it with different vectors in different images.

Computing the Gradient

In this section, let's see how to compute the gradient at a given location. Then, we'll learn how to make a gradient vector by combining its partial derivative in the y and x directions. Gradient vector can be written as partial derivatives of the image in x direction and y direction as shown below.

$$\nabla \mathrm{I} = \left(\frac{\partial I}{\partial x}, \frac{\partial I}{\partial y}\right) \quad \text{.....(3.1)}$$

We can compute the change in intensity of the image with respect to change in value of x using partial derivatives. For continuous functions I(x,y) , it can be written as:

$$\frac{\partial I(x,y)}{\partial x} = \lim_{\Delta x \to 0} \left(\frac{I(x+\Delta x,y) - I(x,y)}{\Delta x}\right) \quad \text{.....(3.2)}$$

There are various algorithms that are used for edge detection. Broadly, they are classified into two categories: derivative based and gradient based. The former takes first and second derivative on each pixel, while the latter takes a gradient in x and y direction for successive pixels. A kernel operation is usually performed when the edge is to be detected[64]

An image gradient is mainly used to identify the regions of the brain that have the most contrast. In MRI scans, the magnitude of the gradient is used to identify the most contrast regions. Due to the presence of outliers in the image, it is challenging to maintain the accuracy of the gradient's prediction. In a study, the researchers found that the image gradient can provide a highly accurate prediction without relying on additional information[65]. Anisotropic diffusion techniques are commonly used to reduce the noise and preserve certain features of an image, such as the edges. According to a study conducted by Beitone et al., the Gradient anisotropic diffusion filter outperforms other methods when it comes to performing global reconstruction errors[66].

A gradient magnitude recursive Gaussian is a type of algorithm that computes the magnitude of an image's gradient by combining the first derivative of a Gaussian through convolution[67]. Gradient-based filters are commonly used in various applications to remove unwanted noise. In a study conducted by Xiaobo Zhang and colleagues, they found that a combination of the signal detection and the local directional variance can reduce the effects of local windows[68].

3.1.2. Brain Extraction

Due to the increasing demand for more accurate and efficient methods for analyzing the brain's magnetic resonance volume, the brain extraction process has been gaining attention. This process is very important for developing neuroimaging systems that can accurately identify brain parts and non-brain tissues. [69]

Brain extraction is a crucial step in the development of brain imaging procedures. It can improve the accuracy and speed of diagnosis in various medical applications. Brain extraction is an important step in brain image analysis which extracts whole brain voxels.It removes non-cerebral tissues such as the skull, dura, and scalp from brain images.[70]

This module is used to first register an image of the patient's brain to atlas. It then propagates the mask of the brain to the patient's data. After the brain mask is eroded, it becomes the initial

stage of a refined brain extraction process. The level-set is then evolved to the edge of the skull border and thus results in accurate brain extraction. The brain mask created by the module is used to store the data of the patient.

3.1.3. Brain Volume Refinement

This module is designed to reduce the manual interference in refining the brain volume.It can also improve the accuracy and speed of diagnosis in various medical applications. It helps in reducing errors caused by humans. The objective of this module is to remove the patterns that don't correspond to the brain's borders. It does so through an iterative process that involves evaluating the image's pixel signal intensity levels. As the volume changes become stable, the algorithm stops correcting the boundary of brain.[71].

Following figures show how volume refinement corrects the voxels at boundary. The fig.3.1(a) shows a slice before refinement and fig.3.1(b) shows it after refinement. It can be seen that peaks at boundary (encircled in blue color) in fig.3.1(a) are suppressed in fig.3.1(b) where corresponding voxels are encircled in red color.

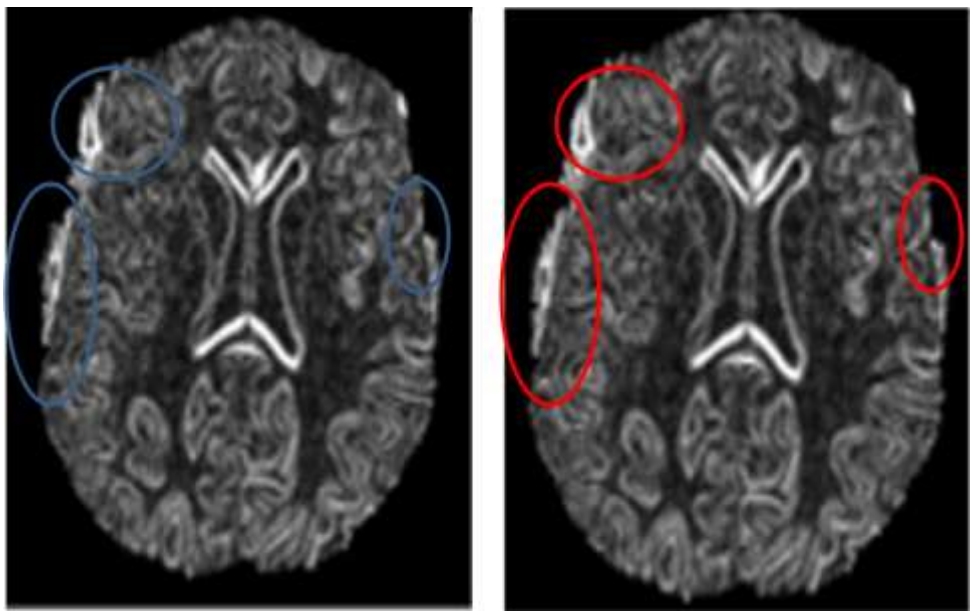

(a) Before Volume Refinement (b) After Volume Refinement

Fig. 3.1: Volume Refinement

3.2. SOURCES OF DATA

3.2.1. Data from Nanavati MAX Superspeciality Hospital, Mumbai

Data of 135 patients of SPGR sequence is obtained from Nanavati Hospital, Mumbai. 86 of them are demented and 49 are non-demented patients.The Committee of the Ethics & Scientific and Clinical Department of the Nanavati MAX Superspeciality Hospital in Mumbai has approved our proposal to conduct this research and collect patient data for the same.

All the images were interpreted by board-certified radiologists with a subspecialty in radiology. The data provided by the hospital is anonymous i.e. no details like Name, financial and educational details of patients are provided. This data is available in DICOM file format and takes approximately 6.4Mb memory space per patient.The GE Medical Systems' MRI machine is used to scan the brain using a magnetic field strength of 3T. The T1 weighted images are acquired through a turbo spin echo sequence. The slice thickness used is 3mm. The acquired images cover a patient's brain in a volume of 230 slices on an average. To validate the segmentation results, we have included an online dataset known as OASIS. Following table 3.1 shows image attributes.

Table 3.1**:** Image Attributes

Attribute Name	**Description**
No. of images per patient	300 approx.
Size of each image	137 KB approx.
Format	DICOM
Width	256
Height	256
Colour type	‘grayscale’

As mentioned above, for MRI data of each patient, around 300 slices are generated. Following fig.3.2 shows slices of MRI of a 65 year old male subject with symptom - forgetfulness. Recorded slices are 330. As it is a huge number, every 10^{th} slice is shown for representational purpose.

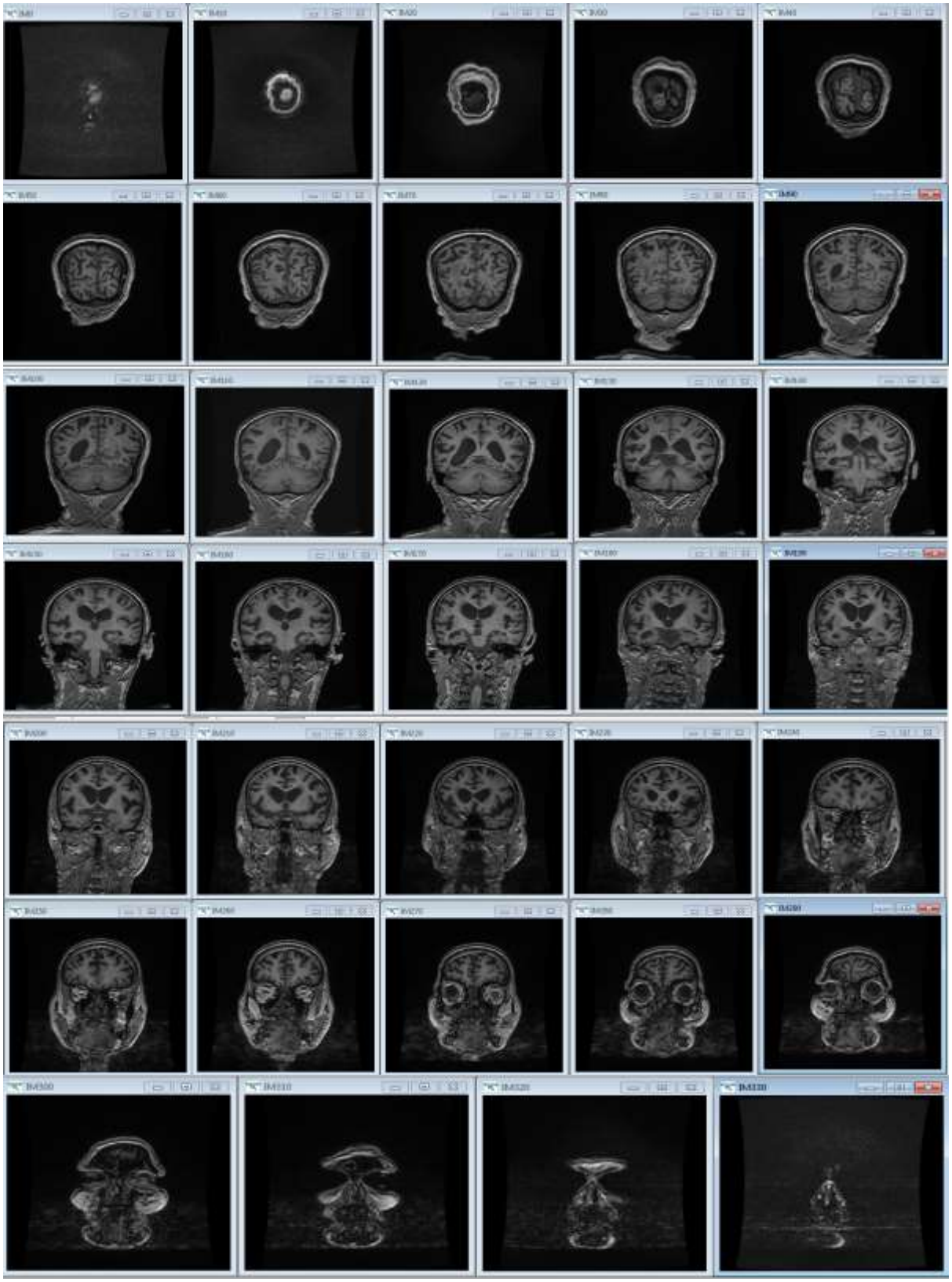

Fig.3.2: MRI volumetric data of a 65 year old male subject

3.2.2. Open Access Series of Imaging Studies (OASIS) Dataset

The OASIS is a community-based platform that allows the public to access a large database of neuroimaging and cognitive data. The collection consists of 150 individuals from 60 to 96 years old. They are scanned on two or more visits, and each session is separated by at least one year. Thus, a total of 373 scans are available.[72].Incomplete data (data with missing values) is not considered for experimentation.

3.3. PROPOSED MODEL FOR INTRACRANIAL VOLUME ESTIMATION

A novel model using Gradient-based filtering is proposed for brain volume estimation. MRI volumetric data is taken as input. Three different gradient-based filters are used for pre-processing. These are the Gradient Magnitude , Gradient Recursive Gaussian and Gradient Anisotropic Diffusion filters. They are used one at a time. The gradient filters help in accurate edge detection. Fig. 3.3 below shows steps involved in proposed model.

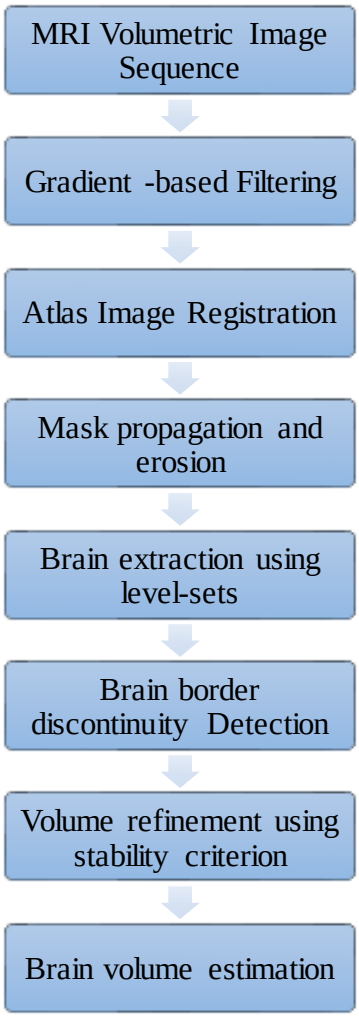

Fig.3.3**:** Proposed Model for Brain Volume Estimation

The next step is registration of atlas image to patient's data. Then the atlas brain mask is applied to patient data. This mask is then eroded and used to perform a refined brain extraction. The level-set is then evolved to the edge of the skull border. The next step improves the segmentation of the brain volume by removing inconsistent patterns. It is based on an iterative evaluation procedure that takes into account the relationship between the local neighborhood and the pixel signal level. The volume stability is the stopping criterion i.e. when the volume change in consecutive iterations becomes stable, it stops brain's boundary correction. Finally , the brain volume is estimated by considering image dimensions through pixel counting. The experimentation is conducted using MATLAB and 3D Slicer [73]. The steps mentioned in above fig. 3.3 were followed for both the datasets i.e. OASIS and Nanavati dataset and results are recorded along with time required for execution.

3.4. PERFORMANCE EVALUATION PARAMETERS

Parameters like Percent Error , Accuracy, Scatter Index and RMSE are used for comparison.

3.5. RESULTS

In the proposed model, the gradient based filtering module is implemented using three different gradient based filters i.e. GMI filter, GMRG filter and GAD filter.

3.5.1. Proposed Model with Gradient Magnitude Image Filter

Result for sample-1

Following fig. 3.4 (a), (b) and (c) show axial coronal and sagittal views of Input image sequence of a patient. Fig. 3.4(d), (e) and (f) show axial coronal and sagittal views of MRI Images after GMIF. Fig.3.4 (g), (h) and (i) show axial coronal and sagittal views of GMIF Images after Brain extraction and Fig.3.4 (j), (k) and (l) show axial coronal and sagittal views of Images after Volume Refinement for a non-demented subject.

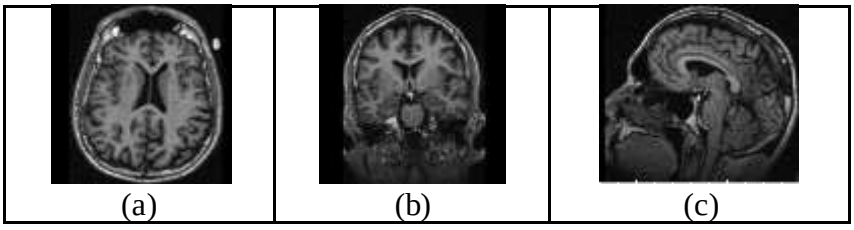

(a) (b) (c)

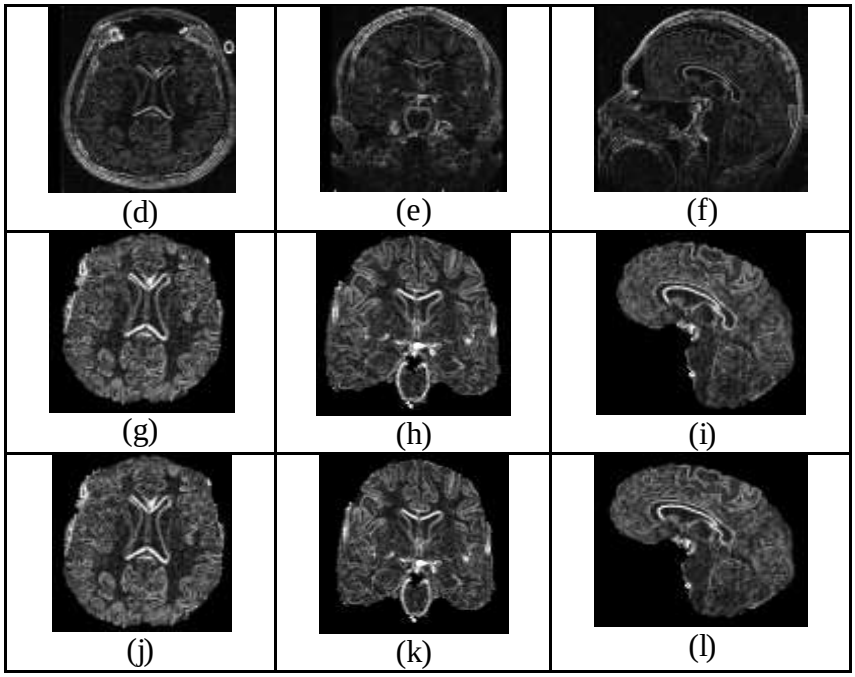

Fig.3.4: Images after execution of different steps in proposed model with GMI Filtering for sample-I

Following table 3.2 shows reference volume, estimated volume using proposed model with GMI filtering and other details.

Table 3.2: Results for Subject OS67 using proposed model with GMI filtering

Patient ID	**OS67**
Group	Non-demented
Gender	F
Age	78
Reference Volume (cm3)	1333
Estimated Volume (cm3)	1332.52
Accuracy (%)	99.93
Error rate	0.07

3.5.2. Proposed Model with Gradient Magnitude Recursive Gaussian Filter

Following fig. 3.5 presents axial coronal and sagittal views from image sequence for a Non-demented 78 year old Female subject at different stages. Fig.3.5 (a),(b) and (c) show input images, fig. 3.5(d), (e), and (f) show images after GMRG filtering, fig. 3.5(g), (h) and (i) show images after brain extraction and Fig. 3.5(j), (k) and (l) show axial coronal and sagittal views of Images after Volume Refinement for a Nondemented subject.

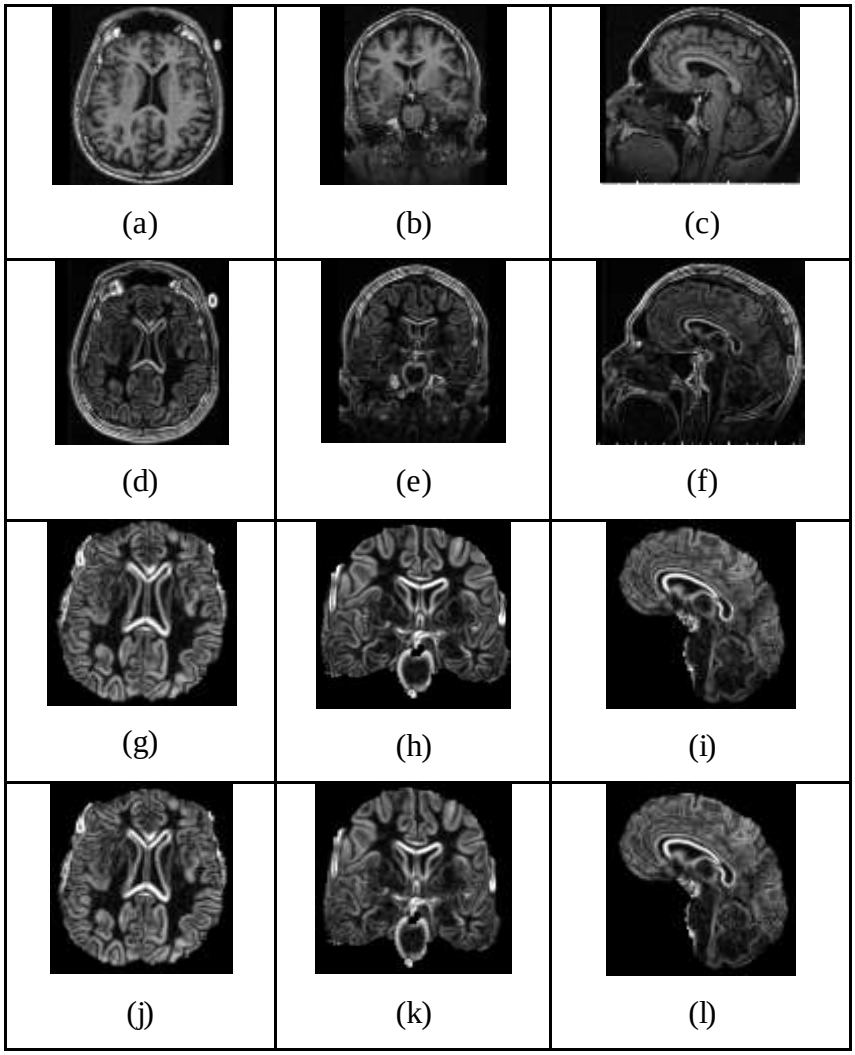

Fig.3.5: Images after execution of different steps in proposed model with GMRG Filtering

Following table 3.3 shows reference volume, estimated volume using proposed model with GMRG filtering and other details.

Table 3.3: Results for Subject OS67 using proposed model with GMRG filtering

Patient ID	**OS67**
Group	Non-demented
Gender	F
Age	78
Reference Volume (cm3)	1333
Estimated Volume (cm3)	1315.27
Accuracy (%)	98.67
Error rate	1.33

3.5.3. Proposed Model with Gradient Anisotropic Diffusion Image Filter

Following fig. 3.6 presents axial coronal and sagittal views from image sequence for a Non-demented 78 year old Female subject at different stages. Fig.3.6 (a),(b) and (c) show input images, fig.3.6 (d), (e), and (f) show images after GAD filtering, fig.3.6 (g), (h) and (i) show images after brain extraction and Fig. 3.6(j), (k) and (l) show axial coronal and sagittal views of Images after Volume Refinement for a Non-demented subject.

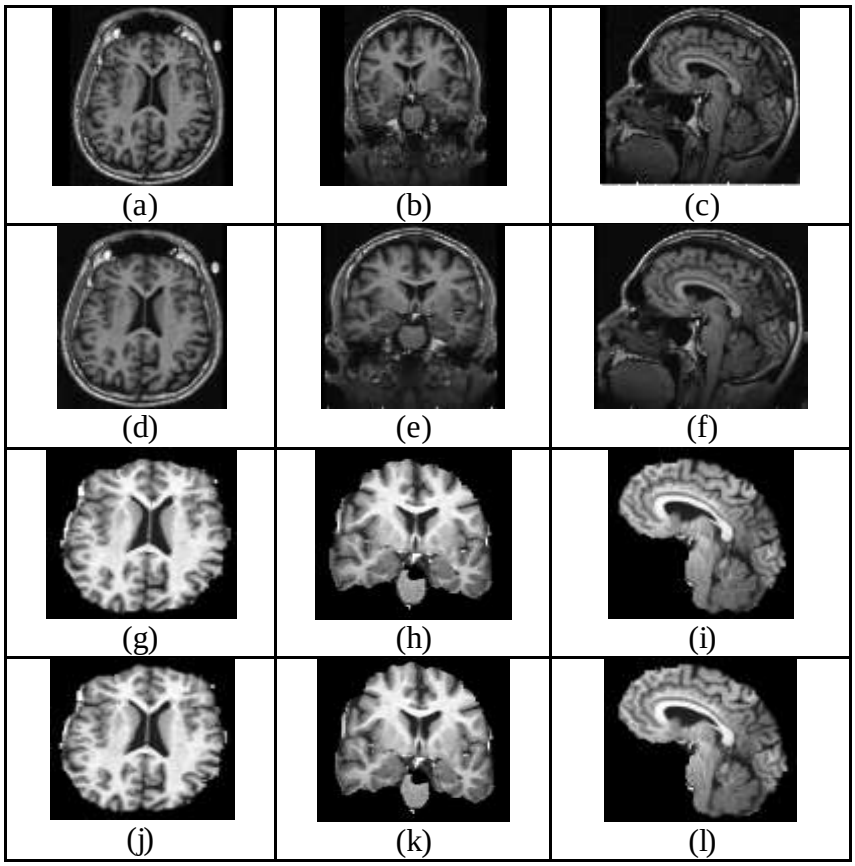

Fig.3.6: Images after execution of different steps in proposed model with GAD Filtering

Following table 3.4 shows reference volume, estimated volume using proposed model with GAD filtering and other details.

Table 3.4: Results for Subject OS67 using proposed model with GAD filtering

Patient ID	**OS67**
Group	Non-demented
Gender	F
Age	78
Reference Volume (cm3)	1333
Estimated Volume (cm3)	1150.512
Accuracy (%)	86.31
Error rate	13.69

3.5.4. Analysis of Results for OASIS Dataset

Following table 3.5 shows Performance evaluation metrics-Accuracy (%), Root Mean Squared error (RMSE) and Scatter Index for Proposed model using OASIS dataset.

Table 3.5 : Performance evaluation metrics for OASIS dataset

Metric	Proposed Model with GMIF	Proposed Model with GMRG	Proposed Model with GAD
Average Accuracy (%)	94.19	91.14	84.4
RMSE	6.9	9.88	16.39
SI	0.49	0.73	1.31

3.5.5. Results for Nanavati Dataset

Following table 3.6 shows Gender-wise count of Subjects in Nanavati dataset used for experimentation

Table 3.6: Gender-wise count of Subjects in Nanavati dataset

Gender/Category	Demented	Nondemented	Total
M	50	26	76
F	36	23	59
Total	86	49	135

Following table 3.7 shows Performance evaluation metrics-Average Accuracy (%), Root Mean Squared error (RMSE) and Scatter Index for Proposed model using Nanavati dataset.

Table 3.7 :Performance evaluation metrics for Nanavati dataset

Metric/ Model	Proposed Model with GMIF	Proposed Model with GMRG	Proposed Model with GAD
Average Accuracy (%)	93.45	92.68	83.6
RMSE	7.7	8.6	17
SI	0.57	0.64	1.4

3.5.6. Comparative analysis for ICV estimation

Following Fig.3.7 shows Brain Volume Estimation Accuracies of proposed models using both the datasets. The model performs well on both the datasets with close values of accuracy.

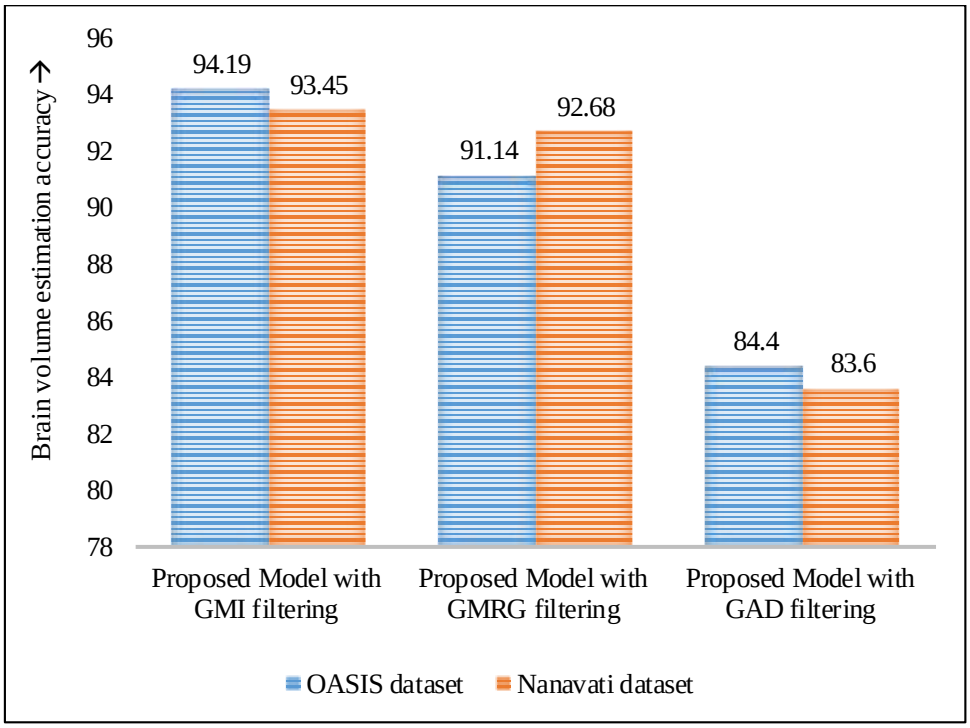

Fig.3.7: Brain Volume Estimation Accuracies of proposed models using OASIS and Nanavati Hospital Data

Following Fig.3.8 shows Root Mean Square Errors of proposed models using both the datasets. Proposed model with GMI filtering gives the least RMSE.

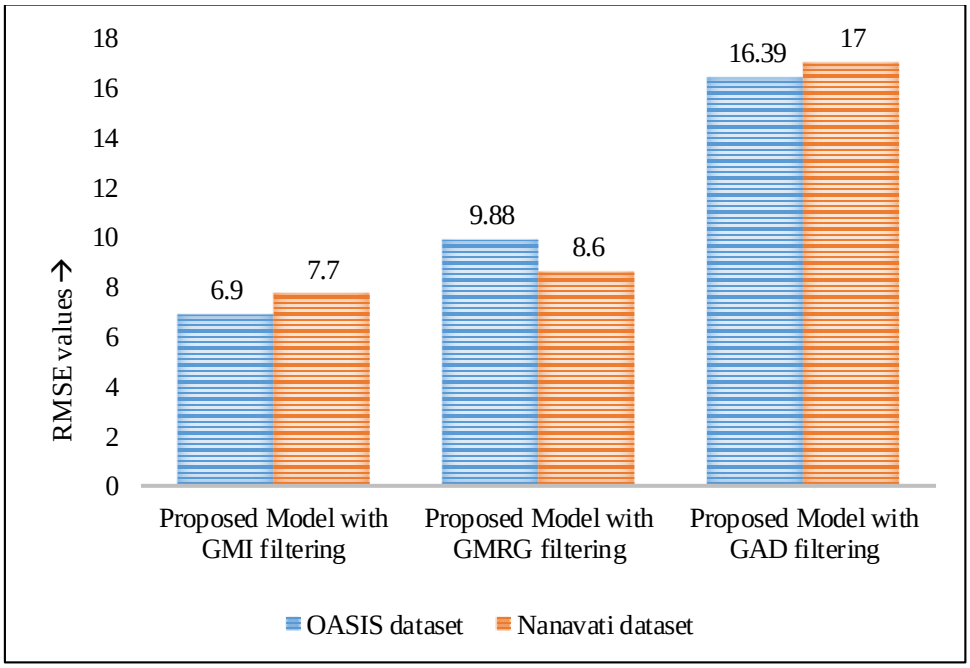

Fig.3.8: Root Mean Square Errors of proposed models using OASIS and Nanavati Hospital Data

Following Fig.3.9 shows Scatter Indices of proposed models using both the datasets. Proposed model with GMI filtering gives the least values of Scatter Indices.

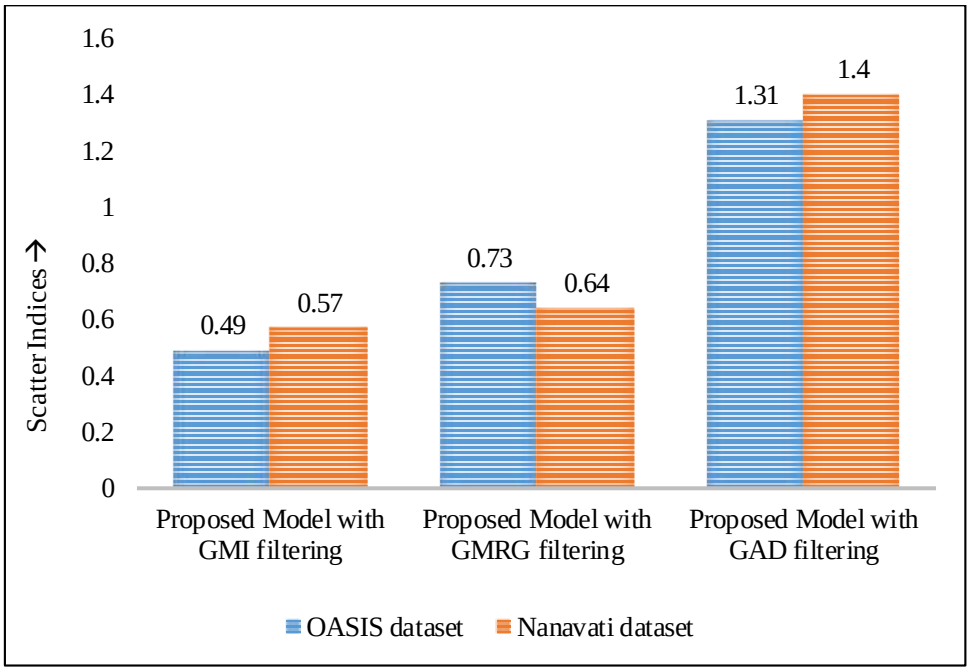

Fig.3.9: Scatter Indices of proposed models using OASIS and Nanavati Hospital Data

Following Fig.3.10 shows Average ICV estimation time using proposed model for both the datasets. On an average, OASIS dataset takes relatively low execution time for ICV estimation.

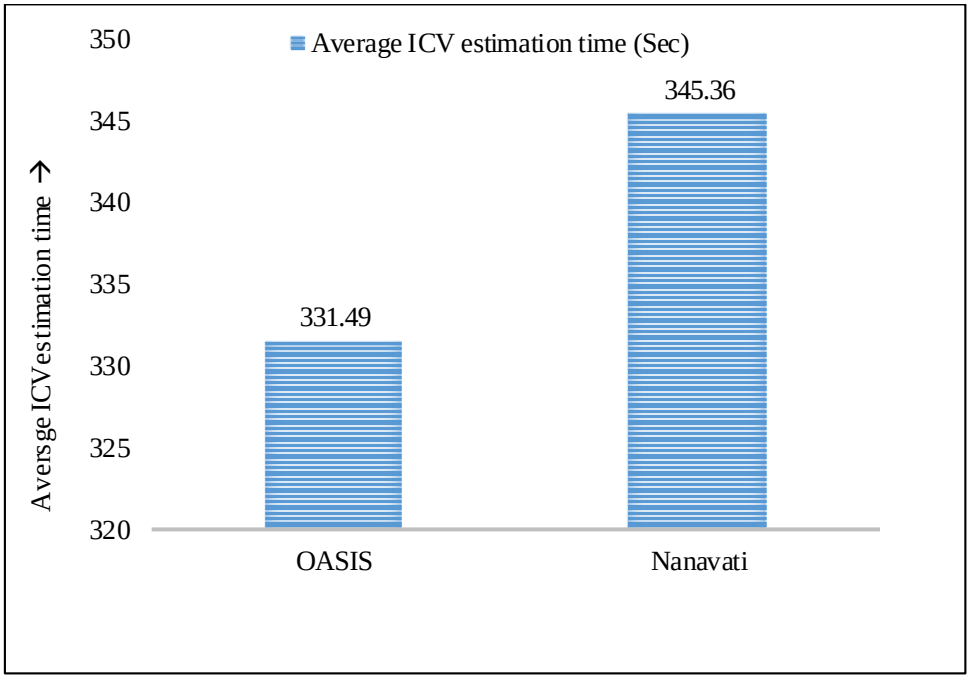

Fig.3.10: Average ICV estimation time using proposed models for OASIS and Nanavati Hospital Data

Following fig. 3.11 shows comparison of proposed models with existing methods of brain volume estimation. Results show that proposed model with GMIF performs the best.

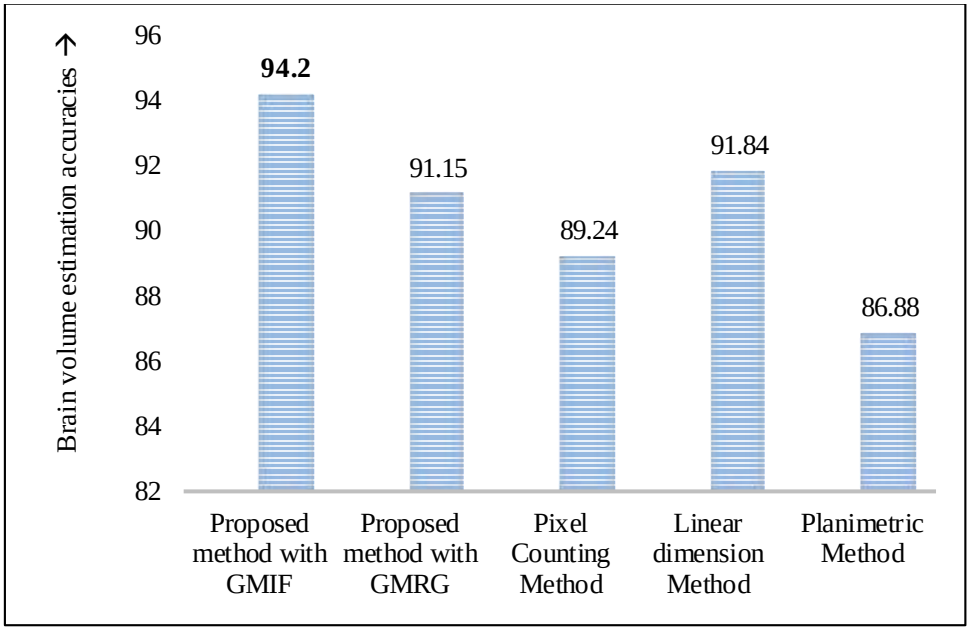

Fig. 3.11: Comparison of proposed model with other methods for estimation of brain volume

3.6. SUMMARY

i) The proposed model performed best with the GMI filter on the OASIS dataset. It had an average accuracy of 94.19% .The proposed model with GMRG and GAD filtering also performed well with an average accuracy of 91.14% and 84.4% respectively.

ii)The proposed model performed well with the Nanavati dataset, giving it an average accuracy of 93.45% , 92.68% and 83.6% with GMI, GMRG and GAD filters respectively.

CHAPTER 4
ESTIMATION OF TOTAL BRAIN VOLUME

4.1. INTRODUCTION

The accurate segmentation is a fundamental concern in medical image analysis. In MRI, the intensity inhomogeneity is a phenomenon that affects the varying intensity of the tissue in the image domain. It can be attributed to various factors such as patient-specific interactions and B1 and B0 field inhomogeneities. Due to the nature of the inhomogeneity, the overlapping ranges of tissues in the image domain can lead to misclassification. This issue can also affect the performance of image registration and other image analysis tools. In order to remove the inhomogeneity from the data, a procedure known as bias field correction is usually performed.

In order to perform a bias field correction, an estimate of the intensity of the inhomogeneity is made by estimating the bias field. Then, a segmentation algorithm is used to divide the image into two parts and generate a biased field corrected image. Unfortunately, most segmentation algorithms fail when the inhomogeneity is present in the images. To perform this procedure, one has to perform a separate preprocessing step.An advanced segmentation algorithm can handle the intensity inhomogeneities without the need for a separate preprocessing step. This method can be used to perform segmentation without the need for a bias field correction. Usually, these methods use an iterative process to perform the segmentation. In the past two decades, numerous techniques have been proposed for performing bias field correction in medical imaging.

There are two types of bias correction techniques that are commonly used in medical imaging: retrospective and prospective methods. The former aims to avoid the intensity inhomogeneity during the acquisition process, while the latter can correct some of the inhomogeneities that occur due to the use of a scanner. Unfortunately, these methods are not able to effectively handle the inhomogeneities in the images that are dependent on patient. Unlike the prospective methods, retrospective techniques rely on the information collected during the acquisition process to identify the inhomogeneities. This method can be performed to remove the intensity in the images that are affected by the patient[74].

4.2. PROPOSED MODEL FOR ESTIMATION OF TOTAL BRAIN VOLUME

The basic idea of this module is to minimize the intensity inhomogeneity in images by correcting the bias field so that better tissue segmentation can be achieved. The first step is to preprocess the images for better segmentation of boundary tissues by correct edge detection. For this purpose, gradient based filters i.e. GMIF and GMRGIF are used. Following fig. 4.1 shows the steps in proposed model for estimation of total brain volume.

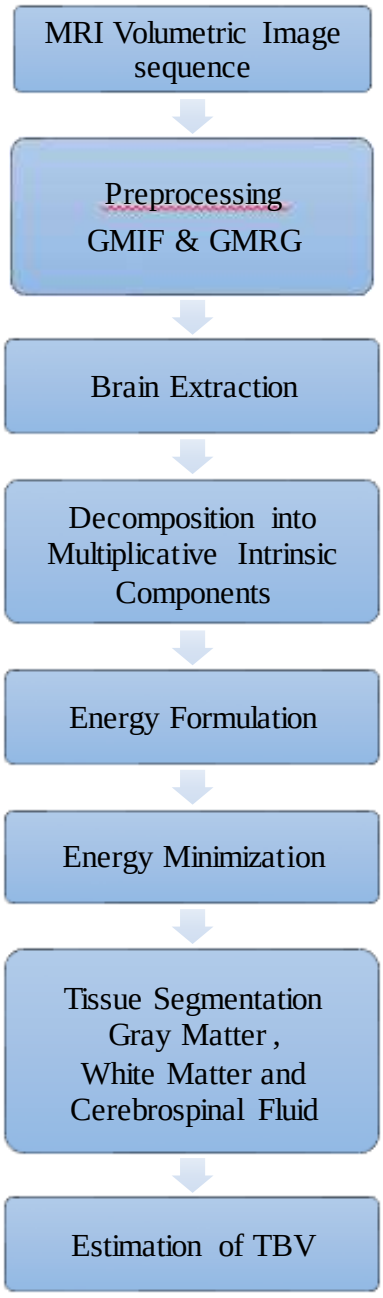

Fig. 4.1: Proposed model for estimation of Total Brain Volume

Later on Brain extraction followed by tissue segmentation is performed. This module decomposes an Magnetic Resonance image sequence into two multiplicative intrinsic components. For optimization of these components, a step to minimize the energy is proposed which results in better tissue segmentation in terms of Gray Matter (GM) ,White Matter (WM) and Cerebrospinal Fluid (CSF). Finally, Total Brain Volume is calculated by adding Gray Matter and White Matter. The experimentation is performed on Nanavati Hospital data and OASIS dataset.

4.3. RESULTS

Results of sample subject-1

Following fig. 4.2 (a), (b) and (c) show axial coronal and sagittal views of Input image sequence of a patient. Fig. 4.2(d), (e) and (f) show axial coronal and sagittal views of MRI Images after GMIF. Fig.4.2 (g), (h) and (i) show axial coronal and sagittal views of GMIF Images after Brain extraction and Fig.4.2 (j), (k) and (l) show axial coronal and sagittal views of Images after Tissue segmentation for a non-demented subject.

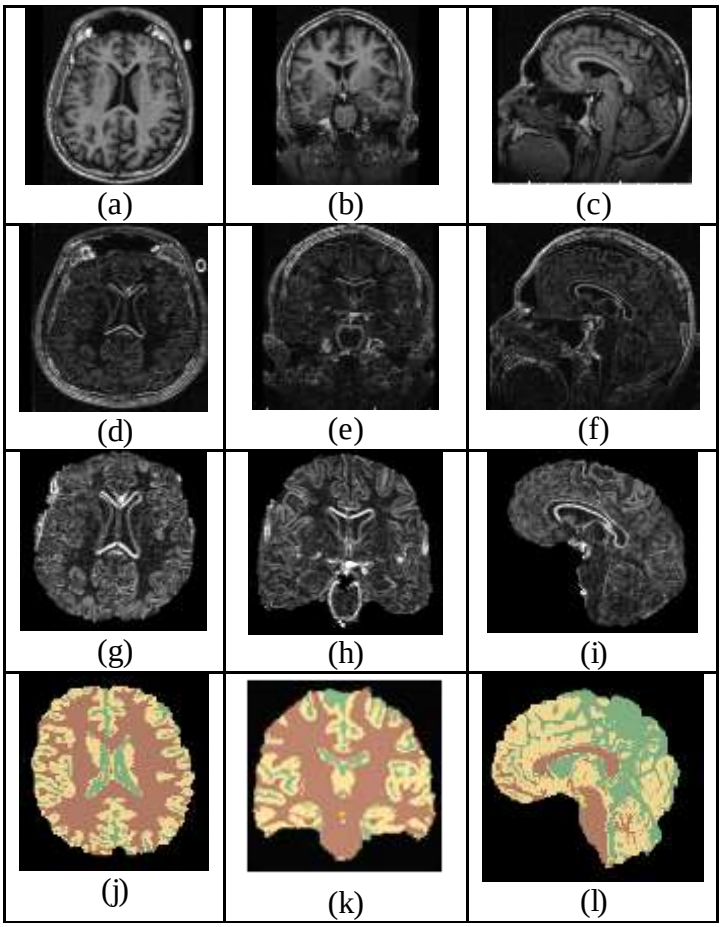

Fig.4.2: Images after execution of different steps in proposed model with GMI Filtering for sample-I

Following table 4.1 shows Results of proposed model for TBV estimation for subject OS67

Table 4.1: Results of proposed model for TBV estimation for subject OS67

Patient ID	**OS67**
Group	Non-demented
Gender	F
Age	78
Reference Volume (cm3)	997
Estimated Volume (cm3)	883.01
Accuracy (%)	88.55
Error rate	11.45

Following table 4.2 shows Performance evaluation metrics-Accuracy (%), Root Mean Squared error (RMSE) and Scatter Index for Proposed model using OASIS dataset.

Table 4.2 : Performance evaluation metrics for OASIS dataset

Metric/Model	**Proposed Model with GMIF**	**Proposed Model with GMRG**
Average Accuracy	91.81	85.16
RMSE	9.32	10.13
SI	0.01	0.01

Following table 4.3 shows Performance evaluation parameters for proposed models using Nanavati dataset

Table 4.3: Performance evaluation parameters for proposed models using Nanavati dataset

Metric/Model	**Proposed Model with GMIF**	**Proposed Model with GMRG**
Average Accuracy	88.28	84.27
RMSE	12.65	10.08
SI	0.01	0.01

4.4. COMPARATIVE ANALYSIS OF RESULTS

Following fig. 4.3 shows comparison of TBV estimation accuracies by proposed models with MICO using both the datasets. Both the proposed models perform better than MICO algorithm. Proposed model with GMI filtering performs best.

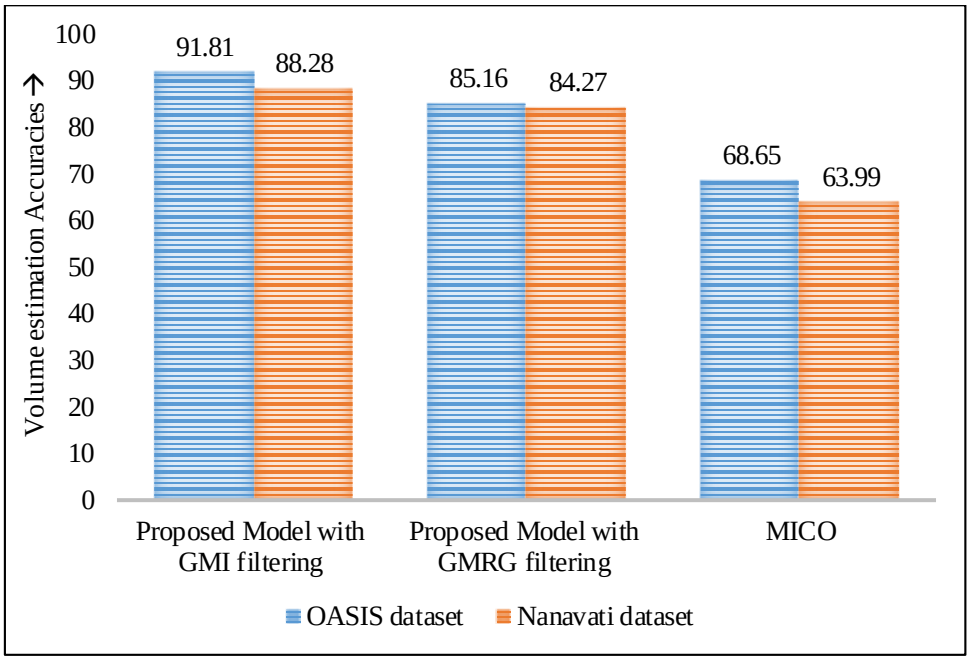

Fig. 4.3: Comparison of TBV estimation accuracies by proposed models with MICO

Following Fig. 4.4 shows comparison of RMSEs of proposed models with MICO using both the datasets. Both the proposed models perform better than MICO algorithm. Proposed model with GMI filtering got the least value of RMSE as 9.32 on OASIS dataset while 10.13 on Nanavati dataset.

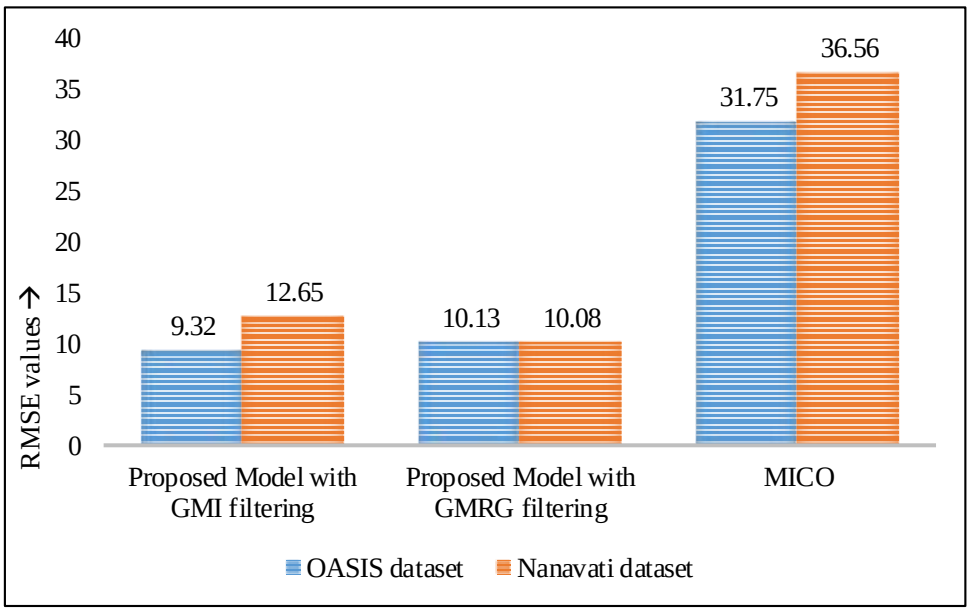

Fig. 4.4: Comparison of RMSEs of proposed models with MICO

Following Fig. 4.5 shows comparison of Scatter Indices of proposed models with MICO using both the datasets. Both the proposed models perform equally and better than MICO algorithm with Scatter Index value 0.01.

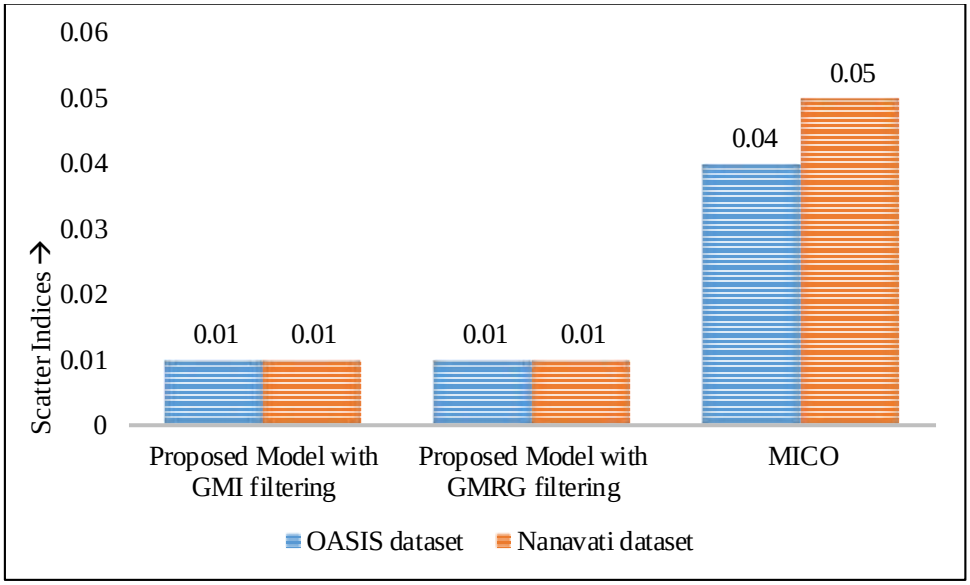

Fig. 4.5: Comparison of Scatter Indices of proposed models with MICO

Following Fig. 4.6 shows comparison of TBV estimation time for Nanavati and OASIS dataset. The proposed model performs faster on OASIS dataset than on Nanavati dataset and on an average takes 263.39 seconds to estimate TBV.

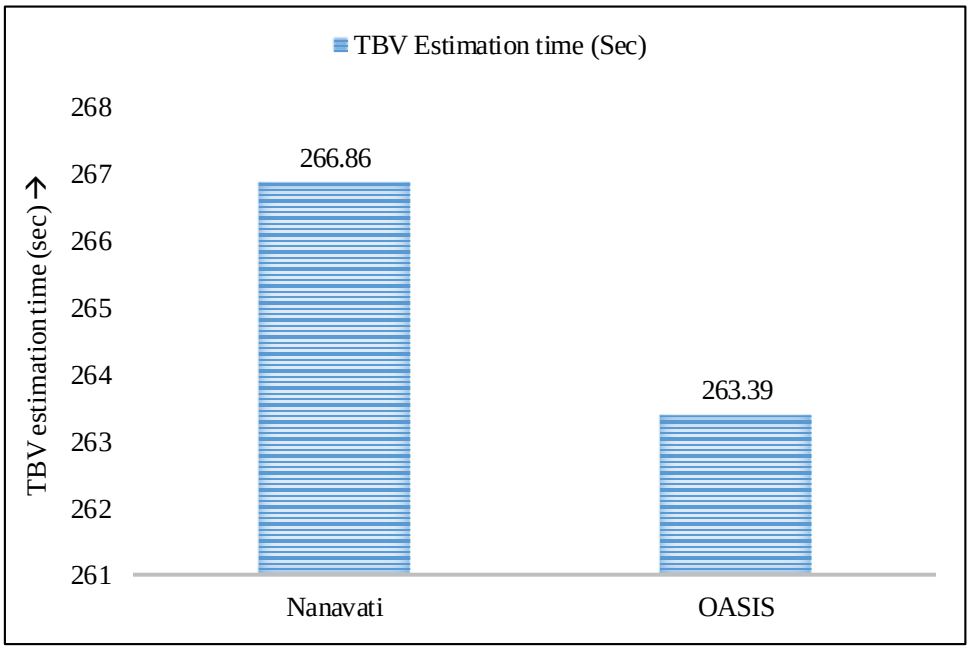

Fig. 4.6: Comparison of TBV estimation time for Nanavati and OASIS dataset

4.5 TIME ESTIMATION OF ICV AND TBV TOGETHER

4.5.1. Total Time required for OASIS data

Following fig. 4.7 shows analysis of estimation time of ICV and TBV individually and in total using both the datasets.

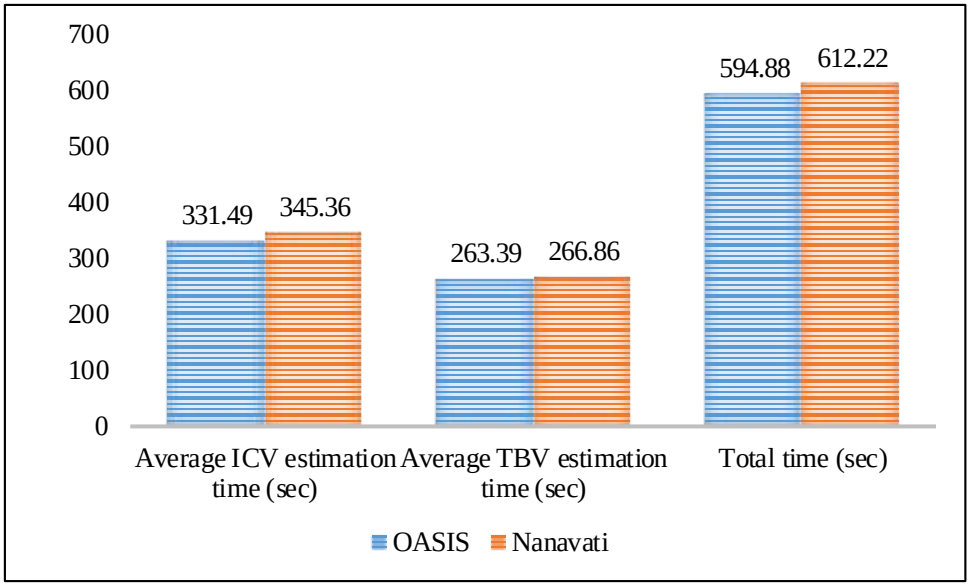

Fig. 4.7: Comparison of estimation time for ICV and TBV together

4.6. SUMMARY

i)Both the proposed models perform better than MICO algorithm.

ii)Proposed model with GMI filtering gives TBV estimation accuracy as 91.81% for OASIS dataset and 88.28% for Nanavati dataset while with GMRG filtering , it gives TBV estimation accuracy as 85.16% for OASIS data and as 84.27% for Nanavati data.

iii)In terms of RMSE, both the proposed models perform better than MICO algorithm. Proposed model with GMI filtering got the least value of RMSE as 9.32 on OASIS dataset while 10.13 on Nanavati dataset.

iv)Both the proposed models perform equally and better than MICO algorithm with Scatter Index value 0.01.

v)The proposed model performs faster on OASIS dataset than on Nanavati dataset and on an average takes 263.39 seconds to estimate TBV.

CHAPTER 5
DEMENTIA CLASSIFICATION

5.1. INTRODUCTION

Dementia is a type of cognitive disorder that generally occurs as a chronic or progressive state. It affects various parts of the brain. Due to the increasing number of people with Dementia in India, the demand for healthcare services is expected to rise significantly. This disease has a negative effect on the quality of life for patients and their families. Early diagnosis of this disease can help in delaying the decline in a patient's abilities and make them more involved in their treatments and decisions. Although no cure has been found for Alzheimer's disease, there are various promising research programs that are focused on finding new ways to treat the disease[75].

5.2. MACHINE LEARNING BASED APPROACHES

5.2.1. Decision Tree

A decision tree method is commonly used to develop classification systems that are based on multiple covariates. It utilizes a population-based approach to classify a group into branch-like segments. This method can handle large datasets without introducing a complex structure. When the sample size gets large enough, the decision tree can be combined with a validation dataset to produce a final model[76].

5.2.2. Logistic Regression

The concept of the logistic regression model is that the odds of an event are divided by the probability that it will not happen. This is done by taking the natural logarithm of the odds and converting it into a function that can be used to predict an outcome[77].

5.2.3. Support Vector Machine

The SVM model is a supervised learning framework that generates separations among groups of observations by mapping them into a higher dimensional space. It does not rely on data distribution and can generate models with great flexibility. The superficial observations which lie on the aforementioned parallel hyperplanes are called support vectors[12]. Different types of functions like Linear, Quadratic, Cubic, Fine Gaussian, Median Gaussian and Coarse Gaussian are used for comparison purpose with proposed model.

5.2.4. Ensemble Learning

One of the most promising research areas in the area of data fusion is ensemble learning, which aims to integrate various data mining and data modeling techniques into a unified framework. It then produces weak predictive results by combining the learned features with multiple learning algorithms. One of the advantages of using bagging techniques is that the accuracy of an ensemble can be tested without removing any data from the training set. [78].

5.3. MORE CLASSIFIERS[79]

The following fig. 5.1 shows the types of classifiers used for comparison, in order to find the best one for our application.

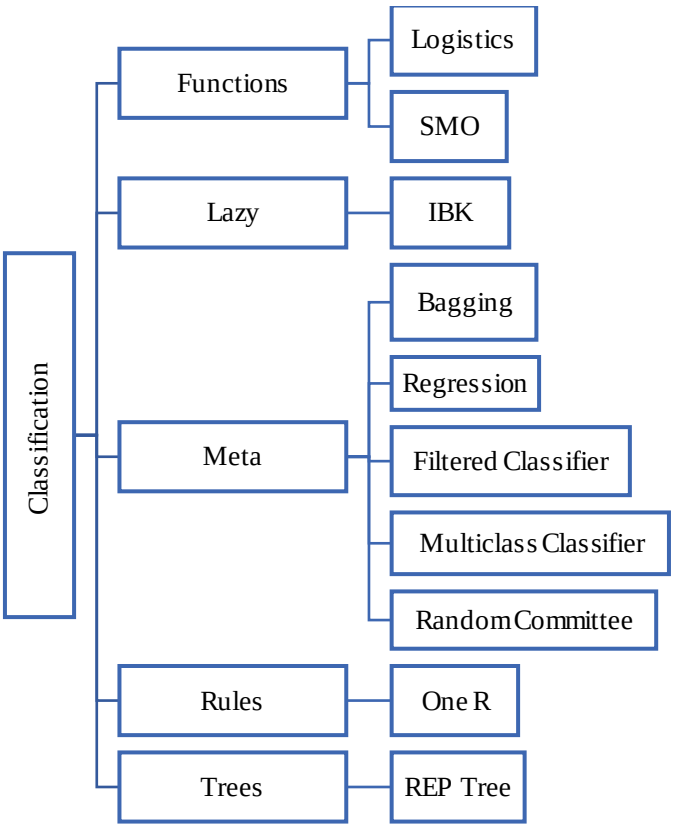

Fig. 5.1: Classifiers used for comparison

5.3.1. Bayesian classifiers

The *NaiveBayes* framework is a probabilistic representation of the Naive Bayes classifier. It can perform various calculations, such as kernel density estimators, on the basis of the normality assumption.The *NaiveBayes Updateable* ,which is an incremental version, can

process one instance at a time. It does not use a kernel estimator.The *NaiveBayes Multinomial* framework is used to implement the multinomial Bayes classifier. The *NaiveBayes-MultinomialText* version, on the other hand, can perform similar calculations on string attributes. *BayesNet* learns Bayesian nets with minimal data attributes, and no missing values.

5.3.2. Tree

With the help of the boosting methods described in this article, the *DecisionStump* can build one-level decision trees for datasets with categorical or numeric classes. It treats the missing values as a separate value and extends the tree's third branch. *RandomTree* constructs random forests by considering the various random features at each node. *RandomForest* then aggregates these random trees into its own random forests. A decision tree or regression tree is built using *REPTree*. It's designed to reduce its errors and improve its speed by splitting instances into smaller pieces. When building a decision tree or regression tree, *Logistic Model Tree(LMT)* takes into account the various missing values and the numerical and nominal attributes at each node. Using *the LogitBoost* module, it can perform a logistic regression function at a node and then use cross-validation to determine the number of iterations that it should run just once. This method improves the tree's run time and accuracy. The minimal complexity of the tree's design helps it produce a compact structure. The *HoeffdingTree* module allows users to split a decision tree into multiple parts by considering the various information gains and the Gini index. It can also predict the leaves using naive Bayes models or majority class models.

5.3.3. Rules

OneR classifies using one parameter. For discretization ,it uses minimum bucket size . Partial decision tree builder *Part* compiles rules from C4.5's heuristics. It generates rules,number of instances covered and number of misclassified instances. *DecisionTable* uses best-first search and cross-validation to evaluate feature subsets. It can also determine the class of instances that are not covered by the entry in the decision table. With the nearest-neighbor method, it can also determine the class of instances that are not covered by the global majority.Using Ripper algorithm and rule set optimization, *JRip* is implemented.

5.3.4. Functions

The *Simple Logistic* framework builds logistic regression models by fitting them to *LogitBoost* and allowing them to perform multiple iterations using cross-validation. It also generates a

robust tree with a single node.The Sequential Minimal Optimization (*SMO)* algorithm is used to train support vector classification using a sequential minimal optimization scheme.

5.3.5. Lazy classifiers

The lazy learner is composed of training instances that do not require real work until the classification time. *IBk* is one of the simplest implementations of the k-nearest-neighbor algorithm. Distance for finding nearest neighbor can be Manhattan, Chebyshev or Minkowski distance.

5.3.6. Metalearning algorithms

A metalearning algorithm takes a classifier and turns it into a powerful learner. One of the parameters that it takes into account is the number of iterations that the system should perform for various iterative schemes, such as boosting and bagging. *FilteredClassifier* classifies filtered data. Filter's own set of parameters, are based on the training data. *Bagging* is a method that reduces the variance in the results of a given classification. It can be used for both regression and classification, since the predictions are based on the average probability estimates. One of the parameters that the algorithm takes into account is the size of the bags. The *RandomCommittee* constructs an ensemble of base classifiers that are based on the same data but use different random number seed. This ensures that the predictions are the same regardless of the base classification.

The *MultiScheme* algorithm selects a classifier to be used from among the various options by using either cross-validation or resubstitution error on the training data. The performance of the regression model is measured by the mean squared error and of classification , by percentage correct.

5.4. RESULTS

5.4.1. Results of Comparison-I

Following table 5.1 summarizes accuracies of different machine learning based Dementia prediction models with *n* fold cross validation. The experimentation is performed using MATLAB classification Learner module on OASIS dataset with 12 attributes.

Table 5.1: Accuracies of Dementia Prediction Models

Model name	Model type : preset	Accuracy % by 4 fold Cross validation	Accuracy % by 5 fold Cross validation	Accuracy % by 10 fold Cross validation
Tree	Fine/Medium/ Coarse Tree	90.3	93.8	96.5
Logistic regression	Logistic regression	87.1	91.6	92.2
SVM	Cubic	83.8	87.3	88.9
SVM	Quadratic	83.3	86.8	88.1
SVM	Linear	82.2	85.4	87.1
SVM	Fine Gaussian	61.7	59.8	62.8
SVM	Medium Gaussian	81.9	85.4	87.1
SVM	Coarse Gaussian	82.2	85.4	87.1
Ensemble	Bagged Trees	97.8	97.3	97.6
Ensemble	Boosted Trees	51.2	51.2	51.2
Ensemble	RUS Boosted Trees	74.1	61.2	70.1

Based on above comparison, it can be stated that Ensemble model with Bagged Trees performs the best with an accuracy of 97.8%. The model is validated best with four- folds. Hence, it can be inferred that there is no more training required for the model.

5.4.2. Results of Comparison-II

To identify the best algorithm for dementia prediction, the experimentation is conducted using OASIS Longitudinal data on Weka tool version 3.9.6. Best 10 classification algorithms are used for comparison and analysis. Table 5.2 below shows detailed results for top ten methods giving best classification accuracies.

Table 5.2: Detailed classification results

Classifier	Time Taken (Sec.)	% of Correctly Classified Instances	% of Incorrectly Classified Instances	Kappa statistic	Mean absolute error	Root mean squared error	Relative absolute error
Ibk	0	98.93%	1.07%	0.9815	0.011	0.0843	2.86%
SMO	0.26	98.66%	1.34%	0.9767	0.2252	0.2776	58.41%
Logistics	0.01	98.39%	1.61%	0.972	0.0107	0.1028	2.78%
Multiclass Classifier	0.2	98.39%	1.61%	0.972	0.0089	0.0792	2.32%
Regression	0.64	97.86%	2.14%	0.9627	0.0231	0.1056	5.98%
One R	0.1	97.86%	2.14%	0.9627	0.0143	0.1196	3.71%
REP Tree	0.01	97.86%	2.14%	0.9627	0.0175	0.0904	4.53%
Bagging	0.09	97.59%	2.41%	0.958	0.1085	0.1613	28.14%
Filtered Classifier	0.09	97.59%	2.41%	0.958	0.1085	0.1613	28.14%
Random committee	0.03	97.59%	2.41%	0.958	0.1553	0.2001	40.27%

With the help of above table it can be inferred that IBk (Instance based learning with parameter –k) classifier performs the best with a classification accuracy of 98.93%. Table 5.3 given below shows weighted average values of all classes for Precision, Recall, F-Measure, Multi-class classification (MCC), Receiver operating characteristic (ROC) Area and Precision-Recall curve (PRC) Area.

Table5.3: Detailed results with different parameters.

Classifier	**Root relative squared error**	**Precision**	**Recall**	**F-Measure**	**MCC**	**ROC Area**	**PRC Area**
Ibk	19.21%	0.99	0.989	0.989	0.982	0.989	0.981
SMO	63.26%	0.987	0.987	0.986	0.977	0.991	0.978
Logistics	23.44%	0.984	0.984	0.984	0.973	0.995	0.988
Multiclass Classifier	18.04%	0.984	0.984	0.984	0.973	0.999	0.998
Regression	24.07%	0.979	0.979	0.978	0.961	0.999	0.998
One R	27.25%	0.979	0.979	0.978	0.961	0.978	0.966
REP Tree	20.61%	0.979	0.979	0.978	0.961	0.999	0.998
Bagging	36.77%	0.977	0.976	0.976	0.957	0.999	0.999
Filtered Classifier	36.77%	0.977	0.976	0.976	0.957	0.999	0.999
Random committee	45.61%	0.976	0.976	0.976	0.959	1	1

On the basis of above results, it can be said that IBK classifier performs the best in terms of Precision, Recall, F-measure and MCC. Following fig. 5.2 shows the percentages of correctly classified instances for different algorithms.

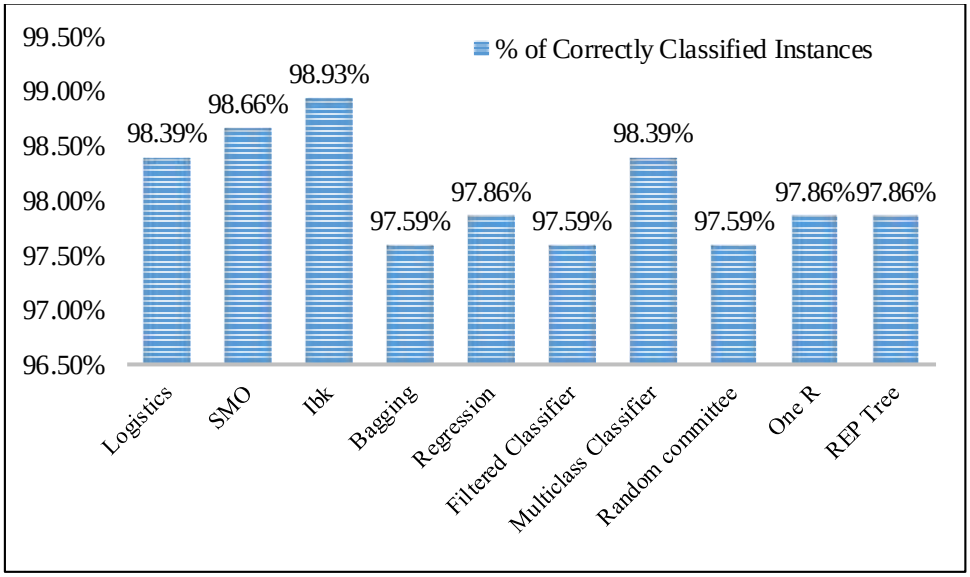

Fig. 5.2: Graph showing Percentages of correctly classified instances with different algorithms using Weka

Fig. 5.3 (a) below shows comparison of True Positive Rates of top 10 algorithms using OASIS dataset. IBK algorithm gives highest True Positive Rate. Fig. 5.3(b) below shows comparison of False Positive Rates of top 10 algorithms using OASIS dataset. IBK algorithm gives lowest False Positive Rate.

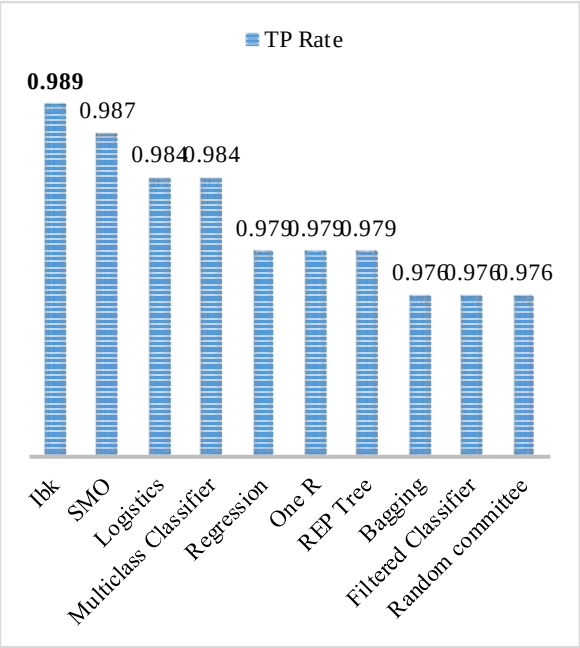

Fig.5.3(a)

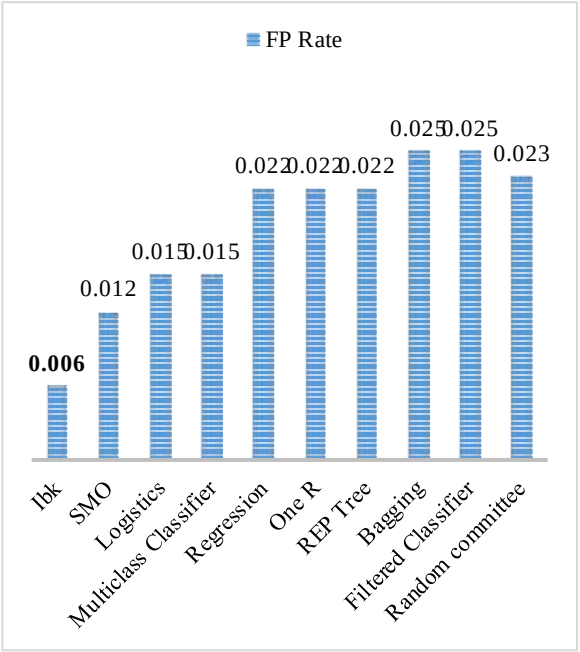

Fig. 5.3(b)

Fig. 5.3: Graphs showing True Positive Rates and False Positive Rates for top 10 algorithms

Following Table 5.4 shows variety of performance evaluation parameters for IBk classifier along with their weighted averages.

Table 5.4: Detailed results of IBk classifier

Performance Evaluation Parameters-> / Class↓	**TP Rate**	**FP Rate**	**Precision**	**Recall**	**F-Measure**	**MCC**	**ROC Area**	**PRC Area**
Non-demented	0.989	0.011	0.989	0.989	0.989	0.979	0.986	0.981
Demented	0.986	0	1	0.986	0.993	0.989	0.991	0.992
Converted	1	0.006	0.949	1	0.974	0.971	0.996	0.933
Weighted Average	**0.989**	**0.006**	**0.99**	**0.989**	**0.989**	**0.982**	**0.989**	**0.981**

Following Table 5.5 shows Confusion Matrix for IBk classifier. Total Number of Instances are 373. Correctly Classified Instances are 369 while Incorrectly Classified Instances are 4.

Table 5.5: Confusion Matrix for IBk classifier

Classified as -> /Class ↓	Non-demented	Demented	Converted
Non-demented	188	0	2
Demented	2	144	0
Converted	0	0	37

5.5. SUMMARY

Experimentation is performed on OASIS longitudinal data set of 150 patients with multiple scans resulting to total 372 records using Weka tool. IBK method performs the best with classification accuracy of 98.93%.

CHAPTER 6
CONCLUSION & FUTURE SCOPE

6.1. CONCLUSION

- In this research, it is tried to develop a model that helps radiologists in estimation of brain volume and hence in prediction of dementia. The proposed model gives appreciable results and saves the time and effort of a radiologist.
- For Intracranial Brain Volume Estimation, the proposed model performed best with the GMI filter on the OASIS dataset. It had an average accuracy of 94.19% .The proposed model with GMRG and GAD filtering also performed well with an average accuracy of 91.14% and 84.4% respectively.
- The proposed model performed well with the Nanavati dataset, giving it an average accuracy of 93.45% , 92.68% and 83.6% with GMI, GMRG and GAD filters respectively.
- In terms of RMSE the proposed model with GMIF perform better than proposed model with GMRG filtering. Proposed model with GMI filtering got the least value of RMSE as 6.9 on OASIS dataset while 7.7 on Nanavati dataset.
- Scatter Indices of the proposed models using GMIF, GMRF and GAD are 0.49,0.73 and 1.31 respectively for OASIS dataset while for Nanavati they are 0.57,0.64 and 1.4 respectively .
- The proposed model performs faster on OASIS dataset than on Nanavati dataset and on an average takes 263.39 seconds to estimate TBV.
- Proposed model with GMI filtering gives TBV estimation accuracy as 91.81% for OASIS dataset and 88.28% for Nanavati dataset while with GMRG filtering , it gives TBV estimation accuracy as 85.16% for OASIS data and as 84.27% for Nanavati data.
- In terms of RMSE, both the proposed models perform better than MICO algorithm. Proposed model with GMI filtering got the least value of RMSE as 9.32 on OASIS dataset while 10.13 on Nanavati dataset.
- Both the proposed models perform equally and better than MICO algorithm with Scatter Index value 0.01.
- The proposed model performs faster on OASIS dataset than on Nanavati dataset and on an average takes 263.39 seconds to estimate TBV.

- On OASIS longitudinal data set of 150 patients and 373 records, IBK method outperforms other methods with classification accuracy of 98.93%.

6.2. FUTURE SCOPE

Currently the dementia prediction model is tested with 13 attributes obtained from OASIS dataset. In future, performance of proposed model can be improved by testing it with other relevant attributes in coordination with radiologists.

PUBLICATIONS

[1] Prashasti Kanikar, Manoj Sankhe and Deepak Patkar, “A Machine Learning based model for Dementia Prediction using MRI”, Jundishapur Journal of Microbiology, Vol. 15, No.1, April 2022, pp.997-1004.

[2] Prashasti Kanikar, Manoj Sankhe and Deepak Patkar, “Volume Estimation from Brain Magnetic Resonance Images using Gradient Filters", NeuoQuantology ,Volume 20,Issue 10, August 2022,pp.9477-9487.

REFERENCES

[1] J. Liu, M. Li, W. Lan, F.-X. Wu, Y. Pan, and J. Wang, "Classification of Alzheimer's Disease Using Whole Brain Hierarchical Network," *IEEE/ACM Trans. Comput. Biol. and Bioinf.*, vol. 15, no. 2, pp. 624–632, Mar. 2018, doi: 10.1109/TCBB.2016.2635144.

[2] E. D. Bigler and D. F. Tate, "Brain Volume, Intracranial Volume, and Dementia:," *Investigative Radiology*, vol. 36, no. 9, pp. 539–546, Sep. 2001, doi: 10.1097/00004424-200109000-00006.

[3] World Health Organization, "Dementia," Oct. 27, 2022. https://www.who.int/news-room/fact-sheets/detail/dementia

[4] J.-P. Thirion and G. Calmon, "Deformation analysis to detect and quantify active lesions in three-dimensional medical image sequences," *IEEE Trans. Med. Imaging*, vol. 18, no. 5, pp. 429–441, May 1999, doi: 10.1109/42.774170.

[5] L. A. Maggio, J. L. Sewell, and A. R. Artino, "The Literature Review: A Foundation for High-Quality Medical Education Research," *J Grad Med Educ*, vol. 8, no. 3, pp. 297–303, Jul. 2016, doi: 10.4300/JGME-D-16-00175.1.

[6] T. Dhollander, "Accounting for Complex Structure in Diffusion Weighted Imaging Data using Volume Fraction Representations," 2014, doi: 10.13140/2.1.3800.2563.

[7] C. R. Noback, Ed., *The human nervous system: structure and function*, 6th ed. Totowa, N.J: Humana Press, 2005.

[8] M. R. Ahmed, Y. Zhang, Z. Feng, B. Lo, O. T. Inan, and H. Liao, "Neuroimaging and Machine Learning for Dementia Diagnosis: Recent Advancements and Future Prospects," *IEEE Rev. Biomed. Eng.*, vol. 12, pp. 19–33, 2019, doi: 10.1109/RBME.2018.2886237.

[9] M. Koziarska-Rościszewska, P. Iwan, G. Kardas, P. Kozarzewski, J. Rysz, and M. Maciejewski, "Influence of selected factors on the prevalence of cognitive disorders and depression among patients over 60 years of age," *fmpcr*, vol. 24, no. 2, pp. 134–138, 2022, doi: 10.5114/fmpcr.2022.115875.

[10] M. Paraskevaidi, P. L. Martin-Hirsch, and F. L. Martin, "Progress and Challenges in the Diagnosis of Dementia: A Critical Review," *ACS Chem. Neurosci.*, vol. 9, no. 3, pp. 446–461, Mar. 2018, doi: 10.1021/acschemneuro.8b00007.

[11] Y. Stern, *Cognitive reserve: theory and applications*. New York: Taylor and Francis, 2007.

[12] G. Tsang, X. Xie, and S.-M. Zhou, "Harnessing the Power of Machine Learning in Dementia Informatics Research: Issues, Opportunities, and Challenges," *IEEE Rev. Biomed. Eng.*, vol. 13, pp. 113–129, 2020, doi: 10.1109/RBME.2019.2904488.

[13] M. M. Patil and A. R. Yardi, "ANN based dementia diagnosis using DCT for brain MR image compression," in *2013 International Conference on Communication and Signal Processing*, Melmaruvathur, India, Apr. 2013, pp. 451–454. doi: 10.1109/iccsp.2013.6577094.

[14] Yo-Ping Huang and S. M. M. Zaza, "A fuzzy approach to evaluating the risk of dementia by analyzing the cortical thickness from MRI," in *2014 IEEE International Conference on System Science and Engineering (ICSSE)*, Shanghai, China, Jul. 2014, pp. 82–87. doi: 10.1109/ICSSE.2014.6887910.

[15] K. A. N. N. P. Gunawardena, R. N. Rajapakse, N. D. Kodikara, and I. U. K. Mudalige, "Moving from detection to pre-detection of Alzheimer's Disease from MRI data," in *2016 Sixteenth International Conference on Advances in ICT for Emerging Regions (ICTer)*, Negombo, Sri Lanka, Sep. 2016, pp. 324–324. doi: 10.1109/ICTER.2016.7829940.

[16] S.-E. Ryu, D.-H. Shin, and K. Chung, "Prediction Model of Dementia Risk Based on XGBoost Using Derived Variable Extraction and Hyper Parameter Optimization," *IEEE Access*, vol. 8, pp. 177708–177720, 2020, doi: 10.1109/ACCESS.2020.3025553.

[17] H. M. T. Ullah, Z. Onik, R. Islam, and D. Nandi, "Alzheimer's Disease and Dementia Detection from 3D Brain MRI Data Using Deep Convolutional Neural Networks," in *2018 3rd International Conference for Convergence in Technology (I2CT)*, Pune, Apr. 2018, pp. 1–3. doi: 10.1109/I2CT.2018.8529808.

[18] E. E. Bron, M. Smits, W. J. Niessen, and S. Klein, "Feature Selection Based on the SVM Weight Vector for Classification of Dementia," *IEEE J. Biomed. Health Inform.*, vol. 19, no. 5, pp. 1617–1626, Sep. 2015, doi: 10.1109/JBHI.2015.2432832.

[19] S. Duchesne, A. Caroli, C. Geroldi, C. Barillot, G. B. Frisoni, and D. L. Collins, "MRI-Based Automated Computer Classification of Probable AD Versus Normal Controls," *IEEE Trans. Med. Imaging*, vol. 27, no. 4, pp. 509–520, Apr. 2008, doi: 10.1109/TMI.2007.908685.

[20] C. Studholme, V. Cardenas, E. Song, F. Ezekiel, A. Maudsley, and M. Weiner, "Accurate Template-Based Correction of Brain MRI Intensity Distortion With Application to Dementia and Aging," *IEEE Trans. Med. Imaging*, vol. 23, no. 1, pp. 99–110, Jan. 2004, doi: 10.1109/TMI.2003.820029.

[21] V. Jain, O. Nankar, D. J. Jerrish, S. Gite, S. Patil, and K. Kotecha, "A Novel AI-Based System for Detection and Severity Prediction of Dementia Using MRI," *IEEE Access*, vol. 9, pp. 154324–154346, 2021, doi: 10.1109/ACCESS.2021.3127394.

[22] R. Raeper, A. Lisowska, and I. Rekik, "Cooperative Correlational and Discriminative Ensemble Classifier Learning for Early Dementia Diagnosis Using Morphological Brain Multiplexes," *IEEE Access*, vol. 6, pp. 43830–43839, 2018, doi: 10.1109/ACCESS.2018.2863657.

[23] A. Basher, B. C. Kim, K. H. Lee, and H. Y. Jung, "Volumetric Feature-Based Alzheimer's Disease Diagnosis From sMRI Data Using a Convolutional Neural Network and a Deep Neural Network," *IEEE Access*, vol. 9, pp. 29870–29882, 2021, doi: 10.1109/ACCESS.2021.3059658.

[24] J. Cheng *et al.*, "Brain Age Estimation From MRI Using Cascade Networks With Ranking Loss," *IEEE Trans. Med. Imaging*, vol. 40, no. 12, pp. 3400–3412, Dec. 2021, doi: 10.1109/TMI.2021.3085948.

[25] S. Leandrou, S. Petroudi, P. A. Kyriacou, C. C. Reyes-Aldasoro, and C. S. Pattichis, "Quantitative MRI Brain Studies in Mild Cognitive Impairment and Alzheimer's Disease: A Methodological Review," *IEEE Rev. Biomed. Eng.*, vol. 11, pp. 97–111, 2018, doi: 10.1109/RBME.2018.2796598.

[26] Rinck P., *Magnetic Resonance in Medicine-The Basic Textbook of the European Magnetic Resonance Forum*, 11th edition. 2017.

[27] S. Kumar, I. Oh, S. Schindler, A. M. Lai, P. R. O. Payne, and A. Gupta, "Machine learning for modeling the progression of Alzheimer disease dementia using clinical data: a systematic literature review," *JAMIA Open*, vol. 4, no. 3, p. ooab052, Jul. 2021, doi: 10.1093/jamiaopen/ooab052.

[28] Saman Sargolzaei 1, Arman Sargolzaei 1, Mercedes Cabrerizo 1, Gang Chen 2, Mohammed Goryawala 1, Alberto Pinzon-Ardila 3, Sergio M Gonzalez-Arias 3 4, Malek Adjouadi, "Estimating Intracranial Volume in Brain Research: An Evaluation of Methods", doi: 10.1007/s12021-015-9266-5.

[29] S. Mehta, T. J. Grabowski, Y. Trivedi, and H. Damasio, "Evaluation of voxel-based morphometry for focal lesion detection in individuals," *NeuroImage*, vol. 20, no. 3, pp. 1438–1454, Nov. 2003, doi: 10.1016/S1053-8119(03)00377-X.

[30] Hikaru TAKEUCHI and Ryuta KAWASHIMA, "Special Feature: Voxel-Based Morphometry—What We Can Know from Volume." May 01, 2017. doi: 10.11477/mf.1416200781.

[31] Henrike Wolf,Per Julin,Hermann-Josef Gertz,Bengt Winblad,Lars-Olof Wahlund, “Intracranial volume in mild cognitive impairment, Alzheimer’s disease and vascular dementia: evidence for brain reserve?”, doi: https://doi.org/10.1002/gps.1205.

[32] Karen J. Ferguson PhD,Joanna M. Wardlaw FRCR, FRCPE,C. Louise Edmond BSc, MB, ChB,Ian J. Deary PhD, FRCPE, FRSE,Alasdair M. J. MacLullich MRCP, PhD, “Intracranial Area: A Validated Method for Estimating Intracranial Volume”, doi: https://doi.org/10.1111/j.1552-6569.2005.tb00289.x.

[33] J. Eritaia *et al.*, “An optimized method for estimating intracranial volume from magnetic resonance images,” *Magn. Reson. Med.*, vol. 44, no. 6, pp. 973–977, Dec. 2000, doi: 10.1002/1522-2594(200012)44:6<973::AID-MRM21>3.0.CO;2-H.

[34] I. Driscoll *et al.*, “Longitudinal pattern of regional brain volume change differentiates normal aging from MCI,” *Neurology*, vol. 72, no. 22, pp. 1906–1913, Jun. 2009, doi: 10.1212/WNL.0b013e3181a82634.

[35] N. Klasson, E. Olsson, C. Eckerström, H. Malmgren, and A. Wallin, “Estimated intracranial volume from FreeSurfer is biased by total brain volume,” *Eur Radiol Exp*, vol. 2, no. 1, p. 24, Dec. 2018, doi: 10.1186/s41747-018-0055-4.

[36] Ridgway, GR; Barnes, J; Pepple, T; Fox, N;, “Estimation of total intracranial volume - a comparison of methods”, [Online]. Available: https://discovery.ucl.ac.uk/id/eprint/1315736

[37] RichardNordenskjöldaFilipMalmbergabElna-MarieLarssonaAndrewSimmonscgSamantha J.BrooksdLarsLindeHåkanAhlströmaLarsJohanssonafJoelKullberg, “Intracranial volume estimated with commonly used methods could introduce bias in studies including brain volume measurement”, doi: https://doi.org/10.1016/j.neuroimage.2013.06.068.

[38] Hassan Khastavaneh; Hossein Ebrahimpour-Komleh, “Brain extraction using isodata clustering algorithm aided by histogram analysis.” doi: 10.1109/KBEI.2015.7436154.

[39] C. Feng, D. Zhao, and M. Huang, “Image segmentation and bias correction using local inhomogeneous iNtensity clustering (LINC): A region-based level set method,” *Neurocomputing*, vol. 219, pp. 107–129, Jan. 2017, doi: 10.1016/j.neucom.2016.09.008.

[40] J. Juntu, J. Sijbers, D. Dyck, and J. Gielen, “Bias Field Correction for MRI Images,” in *Computer Recognition Systems*, vol. 30, M. Kurzyński, E. Puchała, M. Woźniak, and A. Żołnierek, Eds. Berlin, Heidelberg: Springer Berlin Heidelberg, 2005, pp. 543–551. doi: 10.1007/3-540-32390-2_64.

[41] Y. Xia, Z. Ji, and Y. Zhang, “Brain MRI image segmentation based on learning local variational Gaussian mixture models,” *Neurocomputing*, vol. 204, pp. 189–197, Sep. 2016, doi: 10.1016/j.neucom.2015.08.125.

[42] Zexuan Ji, Yong Xia, Quansen Sun, Qiang Chen, Deshen Xia, and D. D. Feng, “Fuzzy Local Gaussian Mixture Model for Brain MR Image Segmentation,” *IEEE Trans. Inform. Technol. Biomed.*, vol. 16, no. 3, pp. 339–347, May 2012, doi: 10.1109/TITB.2012.2185852.

[43] F. Zhao, “Fuzzy clustering algorithms with self-tuning non-local spatial information for image segmentation,” *Neurocomputing*, vol. 106, pp. 115–125, Apr. 2013, doi: 10.1016/j.neucom.2012.10.022.

[44] S. Yazdani, R. Yusof, A. Karimian, M. Pashna, and A. Hematian, “Correction of intensity nonuniformity in breast MR images,” in *Emerging Trends in Image Processing, Computer Vision and Pattern Recognition*, Elsevier, 2015, pp. 219–229. doi: 10.1016/B978-0-12-802045-6.00014-4.

[45] S. Dai, K. Lu, J. Dong, Y. Zhang, and Y. Chen, “A novel approach of lung segmentation on chest CT images using graph cuts,” *Neurocomputing*, vol. 168, pp. 799–807, Nov. 2015, doi: 10.1016/j.neucom.2015.05.044.

[46] M. M. Abdelsamea, G. Gnecco, and M. M. Gaber, "An efficient Self-Organizing Active Contour model for image segmentation," *Neurocomputing*, vol. 149, pp. 820–835, Feb. 2015, doi: 10.1016/j.neucom.2014.07.052.
[47] T. F. Chan and L. A. Vese, "Active contours without edges," *IEEE Trans. on Image Process.*, vol. 10, no. 2, pp. 266–277, Feb. 2001, doi: 10.1109/83.902291.
[48] Chunming Li, Rui Huang, Zhaohua Ding, J. C. Gatenby, D. N. Metaxas, and J. C. Gore, "A Level Set Method for Image Segmentation in the Presence of Intensity Inhomogeneities With Application to MRI," *IEEE Trans. on Image Process.*, vol. 20, no. 7, pp. 2007–2016, Jul. 2011, doi: 10.1109/TIP.2011.2146190.
[49] S. Kobashi, N. Kamiura, Y. Hata, and M. Ishikawa, "Automatic Robust Threshold Finding Aided by Fuzzy Information Granulation," Oct. 1997. doi: 10.1109/ICIP.1997.648020.
[50] Y. Hata; S. Kobashi; S. Hirano; H. Kitagaki; E. Mori, "Automated segmentation of human brain MR images aided by fuzzy information granulation and fuzzy inference", doi: 10.1109/5326.885120.
[51] Tao Song; Mo M. Jamshidi; Roland R. Lee; Mingxiong Huang, "A Modified Probabilistic Neural Network for Partial Volume Segmentation in Brain MR Image", doi: 10.1109/TNN.2007.891635.
[52] Smitha Sunil Kumaran Nair; K. Revathy, "Quantitative Analysis of Brain Tissues from Magnetic Resonance Images." doi: 10.1109/ICDIP.2009.34.
[53] Stefan Bauer, Pascal P Gratz, Jan Gralla, Mauricio Reyes, Roland Wiest, "Towards automatic MRI volumetry for treatment selection in acute ischemic stroke patients." doi: 10.1109/EMBC.2014.6943891 Abstract.
[54] J. Tohka, A. Zijdenbos, and A. Evans, "Fast and robust parameter estimation for statistical partial volume models in brain MRI," *NeuroImage*, vol. 23, no. 1, pp. 84–97, Sep. 2004, doi: 10.1016/j.neuroimage.2004.05.007.
[55] "RP-Net: A 3D Convolutional Neural Network for Brain Segmentation From Magnetic Resonance Imaging", doi: 10.1109/ACCESS.2019.2906890.
[56] S. S. Keller *et al.*, "Volume Estimation of the Thalamus Using Freesurfer and Stereology: Consistency between Methods," *Neuroinform*, vol. 10, no. 4, pp. 341–350, Oct. 2012, doi: 10.1007/s12021-012-9147-0.
[57] R. Marcos, R. A. F. Monteiro, and E. Rocha, "The use of design-based stereology to evaluate volumes and numbers in the liver: a review with practical guidelines: Design-based stereology in hepatology," *Journal of Anatomy*, vol. 220, no. 4, pp. 303–317, Apr. 2012, doi: 10.1111/j.1469-7580.2012.01475.x.
[58] S. Singhal *et al.*, "Simplifying Tumor Volume Estimation from Linear Dimensions for Intra-Cranial Lesions Treated with Stereotactic Radiosurgery," *J Med Phys*, vol. 45, no. 4, pp. 199–205, Dec. 2020, doi: 10.4103/jmp.JMP_56_20.
[59] K. Nithyakalyani, R. Kalpana, S. Sudhakar, and N. Vigneswaran, "A Novel Pixel Counting Technique to Assess the Volumetric Changes in Human Brain Morphology," *Biosci., Biotechnol. Res. Asia*, vol. 12, no. 1, pp. 677–685, Apr. 2015, doi: 10.13005/bbra/1712.
[60] T. Priya, P. Kalavathi, V. B. S. Prasath, and R. Sivanesan, "Brain tissue volume estimation to detect Alzheimer's disease in magnetic resonance images," *Soft Comput*, vol. 25, no. 15, pp. 10007–10017, Aug. 2021, doi: 10.1007/s00500-021-05621-8.
[61] D. J. Peck, J. P. Windham, L. L. Emery, H. Soltanian-Zadeh, D. O. Hearshen, and T. Mikkelsen, "Cerebral tumor volume calculations using planimetric and eigenimage analysis," *Med. Phys.*, vol. 23, no. 12, pp. 2035–2042, Dec. 1996, doi: 10.1118/1.597900.
[62] S. Bauer, T. Fejes, and M. Reyes, "A Skull-Stripping Filter for ITK," *The Insight Journal*, Jan. 2013, doi: 10.54294/dp4mfp.

[63] A. Hoopes, J. S. Mora, A. V. Dalca, B. Fischl, and M. Hoffmann, "SynthStrip: skull-stripping for any brain image," *NeuroImage*, vol. 260, p. 119474, Oct. 2022, doi: 10.1016/j.neuroimage.2022.119474.
[64] J. A. M. Saif, M. H. Hammad, and I. A. A. Alqubati, "Gradient Based Image Edge Detection," *IJET*, vol. 8, no. 3, pp. 153–156, Mar. 2016, doi: 10.7763/IJET.2016.V6.876.
[65] W. Xue, L. Zhang, X. Mou, and A. C. Bovik, "Gradient Magnitude Similarity Deviation: A Highly Efficient Perceptual Image Quality Index," *IEEE Trans. on Image Process.*, vol. 23, no. 2, pp. 684–695, Feb. 2014, doi: 10.1109/TIP.2013.2293423.
[66] C. Beitone, X. Balandraud, D. Delpueyo, and M. Grédiac, "Heat source reconstruction from noisy temperature fields using a gradient anisotropic diffusion filter," *Infrared Physics & Technology*, vol. 80, pp. 27–37, Jan. 2017, doi: 10.1016/j.infrared.2016.11.003.
[67] "GRADIENT ADAPTIVE IMAGE RESTORATION AND ENHANCEMENT." doi: doi:10.1109/icip.2006.313034.
[68] X. Zhang and X. Feng, "Hybrid gradient-domain image denoising," *AEU - International Journal of Electronics and Communications*, vol. 68, no. 3, pp. 179–185, Mar. 2014, doi: 10.1016/j.aeue.2013.08.009.
[69] H. Z. U. Rehman, H. Hwang, and S. Lee, "Conventional and Deep Learning Methods for Skull Stripping in Brain MRI," *Applied Sciences*, vol. 10, no. 5, p. 1773, Mar. 2020, doi: 10.3390/app10051773.
[70] S. Roy and P. Maji, "A simple skull stripping algorithm for brain MRI," in *2015 Eighth International Conference on Advances in Pattern Recognition (ICAPR)*, Kolkata, India, Jan. 2015, pp. 1–6. doi: 10.1109/ICAPR.2015.7050671.
[71] A. C. da Silva Senra Filho, F. H. Simozo, and L. O. M. Junior, "Brain volume refinement (BVeR): automatic correction tool as an alternative to manual intervention on brain segmentation," *Research on Biomedical Engineering*, vol. 37, no. 4, pp. 631–640, Dec. 2021, doi: 10.1007/s42600-021-00168-x.
[72] D. S. Marcus, A. F. Fotenos, J. G. Csernansky, J. C. Morris, and R. L. Buckner, "Open Access Series of Imaging Studies: Longitudinal MRI Data in Nondemented and Demented Older Adults," *Journal of Cognitive Neuroscience*, vol. 22, no. 12, pp. 2677–2684, Dec. 2010, doi: 10.1162/jocn.2009.21407.
[73] A. Fedorov *et al.*, "3D Slicer as an image computing platform for the Quantitative Imaging Network," *Magnetic Resonance Imaging*, vol. 30, no. 9, pp. 1323–1341, Nov. 2012, doi: 10.1016/j.mri.2012.05.001.
[74] C. Li, J. C. Gore, and C. Davatzikos, "Multiplicative intrinsic component optimization (MICO) for MRI bias field estimation and tissue segmentation," *Magnetic Resonance Imaging*, vol. 32, no. 7, pp. 913–923, Sep. 2014, doi: 10.1016/j.mri.2014.03.010.
[75] K. Trojachanec, I. Kitanovski, I. Dimitrovski, and S. Loshkovska, "Longitudinal Brain MRI Retrieval for Alzheimer's Disease Using Different Temporal Information," *IEEE Access*, vol. 6, pp. 9703–9712, 2018, doi: 10.1109/ACCESS.2017.2773359.
[76] Y.-Y. Song and Y. Lu, "Decision tree methods: applications for classification and prediction," *Shanghai Arch Psychiatry*, vol. 27, no. 2, pp. 130–135, Apr. 2015, doi: 10.11919/j.issn.1002-0829.215044.
[77] M. P. LaValley, "Logistic Regression," *Circulation*, vol. 117, no. 18, pp. 2395–2399, May 2008, doi: 10.1161/CIRCULATIONAHA.106.682658.
[78] R. E. Banfield, L. O. Hall, K. W. Bowyer, and W. P. Kegelmeyer, "A Comparison of Decision Tree Ensemble Creation Techniques," *IEEE Trans. Pattern Anal. Mach. Intell.*, vol. 29, no. 1, pp. 173–180, Jan. 2007, doi: 10.1109/TPAMI.2007.250609.
[79] Eibe Frank, Mark A. Hall, and Ian H. Witten, "The WEKA Workbench.Online Appendix for 'Data Mining: Practical Machine Learning Tools and Techniques'Morgan

Kaufmann." 2016. Accessed: Apr. 06, 2022. [Online]. Available: https://www.cs.waikato.ac.nz/ml/weka/Witten_et_al_2016_appendix.pdf